

1
2
3
4
5
6
7
8
9
10
11
12
13
14
15
16
17
18

Enhancer identification and activity evaluation in the red flour beetle, *Tribolium castaneum*

Yi-Ting Lai¹, Kevin D. Deem¹, Ferran Borràs-Castells¹, Nagraj Sambrani¹, Heike Rudolf², Kushal Suryamohan³, Ezzat El-Sherif², Marc S. Halfon³, Daniel J. McKay⁴, and Yoshinori Tomoyasu^{1‡}

¹Department of Biology, Miami University, Oxford OH 45056, ²Friedrich-Alexander-Universität Erlangen-Nürnberg, Erlangen 91058, Germany, ³Department of Biochemistry, State University of New York at Buffalo, Buffalo, NY 14214, ⁴Department of Biology, Department of Genetics, Integrative Program for Biological and Genome Sciences, University of North Carolina at Chapel Hill, Chapel Hill, NC 27599,

[‡]Author for correspondence (tomoyay@miamioh.edu)

19 **ABSTRACT**

20 Evolution of *cis*-properties (such as enhancers) often plays an important role in the
21 production of diverse morphology. However, a mechanistic understanding is often
22 limited by the absence of methods to study enhancers in species outside of
23 established model systems. Here, we sought to establish methods to identify and test
24 enhancer activity in the red flour beetle, *Tribolium castaneum*. To identify possible
25 enhancer regions, we first obtained genome-wide chromatin profiles from various
26 tissues and stages of *Tribolium* via FAIRE (Formaldehyde Assisted Isolation of
27 Regulatory Elements)-sequencing. Comparison of these profiles revealed a distinct
28 set of open chromatin regions in each tissue and stage. Second, we established the
29 first reporter assay system that works in both *Drosophila* and *Tribolium*, using *nubbin*
30 in the wing and *hunchback* in the embryo as case studies. Together, these advances
31 will be useful to study the evolution of *cis*-language and morphological diversity in
32 *Tribolium* and other insects.

33

34 **KEY WORDS:** Enhancer, Reporter assay, *Tribolium*, Chromatin profiling, FAIRE-seq

35

36 INTRODUCTION

37 Insects display some of the greatest diversity of morphology found amongst eukaryotic taxa,
38 offering a variety of opportunities to investigate molecular and developmental mechanisms
39 underlying morphological evolution. Decades of studies in evolutionary developmental
40 biology (evo-devo) have revealed that changes in gene regulatory networks (GRNs) have
41 been a major driving force in the production of the diverse morphology seen in insects as
42 well as in other taxa (Carroll, 2008; Carroll et al., 2005). In general, a GRN can be divided
43 into two components: *trans* and *cis*. *trans* components are transcription factors (TFs) and
44 their upstream regulators (such as signal transduction pathways) that provide instructive cues
45 for patterning and differentiation to the tissues where they are expressed. In contrast, *cis*
46 components are non-coding DNA elements (*i.e.* *cis*-regulatory elements, CREs) that gather
47 and process the upstream *trans* information and determine the spatial and temporal
48 expression of the genes downstream in the genetic pathway. Changes in both *cis* and *trans*
49 components have been implicated in morphological evolution (Carroll, 2008; Carroll et al.,
50 2005; Halfon, 2017).

51 By embracing unparalleled genetic tools, both *cis* and *trans* factors have been
52 analyzed in great detail in the fruit fly, *Drosophila melanogaster*. The accumulated
53 knowledge obtained from *Drosophila* studies can be used as a reference (*i.e.* the *Drosophila*
54 paradigm) when studying other insects and identifying the changes in GRNs responsible for
55 morphological evolution. RNA interference (RNAi)-based gene knock-down techniques have
56 allowed for an investigation of the *trans* properties involved in development and their
57 evolutionary conservation/diversification in various insects (Belles, 2010). However, the lack
58 of a reliable method to identify *cis* properties in non-*Drosophila* insects has made it difficult
59 to study the evolution of *cis* properties beyond *Drosophila* species, even though it is equally
60 important to study *cis* properties to gain a more comprehensive view of changes in GRNs that

61 contributed to morphological evolution.

62 The major difficulty in identifying CREs, such as enhancers, stems from the labile
63 nature of *cis* properties. The genes that code for *trans* factors important for development are
64 usually evolutionarily well-conserved, thus it is relatively easy to identify these *trans*
65 properties in various insects based on their homologies (Carroll et al., 2005). In contrast, *cis*
66 properties appear to be more evolutionarily flexible in a variety of aspects. First, the order of
67 TF binding sites can vary widely within an enhancer region, and the location of enhancers
68 relative to the target gene also appears to be variable. Second, there can be redundancy
69 among multiple enhancers responsible for the same gene (i.e. shadow enhancers) (Hong et al.,
70 2008), allowing them to evolve more rapidly. In addition, the function of each enhancer tends
71 to exhibit low levels of pleiotropy (Carroll, 2008), resulting in the accumulation of more
72 evolutionary changes in enhancers. These characteristics, along with the faster rate of genome
73 evolution in insects compared to vertebrates (Zdobnov and Bork, 2007), make the
74 identification of insect enhancers a challenging task.

75 Traditionally, enhancers have been identified through reporter assays, in which the
76 transcriptional activation capability of genomic regions near the gene of interest are assessed
77 via a reporter gene construct (see (Suryamohan and Halfon, 2015) to review traditional as
78 well as new methods to identify enhancers). This is a time-consuming and arduous approach,
79 as an enhancer can sometimes reside hundreds of thousands of base pairs away from the gene
80 that the enhancer regulates (Shlyueva et al., 2014). Identification of evolutionarily conserved
81 genomic regions outside of coding regions among several closely related species, such as the
82 *Drosophila* species group, has been helpful in narrowing down regions to survey for enhancer
83 activity (phylogenetic footprinting) (Frazer et al., 2004; Mayor et al., 2000; Sosinsky et al.,
84 2007; Stark et al., 2007). Enhancer predictions based on the TF binding motifs have also been
85 helpful in identifying potential enhancer regions, although the prediction appears to work

86 more efficiently for embryonic enhancers due to the clustering tendency of TF binding motifs
87 within an enhancer active during the syncytial blastoderm stage, while enhancers for other
88 stages might be more difficult to identify through current prediction methods (Li et al., 2007).
89 Combinations of these approaches have allowed for successful identification of enhancers
90 that are active in various developmental contexts in *Drosophila*. More recently, the reporter
91 assay approach has been applied in a genome-wide fashion in *Drosophila* (such as The
92 FlyLight project), identifying over ten thousand genomic regions capable of activating
93 transcription (Jenett et al., 2012; Jory et al., 2012; Kvon et al., 2014; Pfeiffer et al., 2008).
94 Unfortunately, many of these approaches are technically demanding and resource-intensive,
95 and thus are currently only possible in *Drosophila* (but also see (Kazemian et al., 2014) for
96 the successful application of enhancer prediction in non-*Drosophila* insects).

97 In parallel to the above methods, several genomic approaches have been developed
98 for the identification of possible enhancer regions in the *Drosophila* genome (reviewed in
99 (Shlyueva et al., 2014; Suryamohan and Halfon, 2015)). One such method is
100 Formaldehyde-Assisted Isolation of Regulatory Elements (FAIRE) in combination with next
101 generation sequencing (FAIRE-seq), which identifies open chromatin regions genome-wide
102 (Simon et al., 2012). FAIRE-seq has been used in *Drosophila*, showing that open chromatin
103 regions often correspond to enhancers and other CREs (McKay and Lieb, 2013; Pearson et al.,
104 2016; Uyehara et al., 2017). In addition, FAIRE-seq requires less input material and does not
105 rely on antibodies, thus making it less technically demanding compared to techniques like
106 Chromatin Immunoprecipitation sequencing (ChIP-seq). These features also make FAIRE a
107 promising technique to apply to non-*Drosophila* insects. However, it is important to note that
108 potential enhancers identified by FAIRE (or other genomic approaches) still require
109 functional validations, such as with a reporter assay. This presents another significant hurdle
110 when studying enhancers in non-*Drosophila* insects, as the availability of a modern genetic

111 toolkit (such as a versatile reporter construct) is very limited outside of the *Drosophila*
112 species.

113 In this study, we set out to establish an enhancer identification and evaluation method
114 in the red flour beetle, *Tribolium castaneum*. *Tribolium* offers a wide variety of genetic and
115 genomic tools, making this insect a powerful model system for comparative developmental
116 biology and evo-devo studies (Denell, 2008; Schmitt-Engel et al., 2015; Tribolium Genome
117 Sequencing et al., 2008; Wang et al., 2007). The robust systemic RNAi response of *Tribolium*
118 has allowed researchers to study *trans* properties in detail (Brown et al., 1999; Bucher et al.,
119 2002; Tomoyasu and Denell, 2004) and identify changes in GRNs responsible for
120 morphological evolution from the *trans* point of view (see (Peel, 2008) to review the findings
121 related to the evolution of insect segmentation; (Tomoyasu et al., 2009) for insect wing
122 evolution; and (Angelini et al., 2012; Smith et al., 2014) for the evolution of insect
123 appendages). However, studies of *cis* properties in *Tribolium* are currently limited due to the
124 lack of reliable enhancer identification methods.

125 For the initial identification of possible enhancer regions, we first implemented
126 FAIRE-seq and obtained genome-wide chromatin profiles from various tissues and stages of
127 *Tribolium*. The comparison of chromatin profiles between different tissues and stages
128 revealed a distinct set of open chromatin regions in each tissue and stage. Overall, the
129 *Tribolium* open chromatin characteristics are similar to that of *Drosophila*, however, we also
130 noticed some features unique to the *Tribolium* chromatin profiles. Comparison of the FAIRE
131 data to the candidate enhancer regions in the *Tribolium* genome predicated by SCRMshaw
132 (Supervised Cis-Regulatory Module) (Kantorovitz et al., 2009; Kazemian et al., 2011;
133 Kazemian et al., 2014) revealed a very high (>75%) overlap between the two datasets. In
134 addition, we compared the FAIRE profile to the two previously reported enhancer analyses in
135 *Tribolium* (Cande et al., 2009; Eckert et al., 2004; Kazemian et al., 2014; Wolff et al., 1998),

136 and found that the enhancers identified in these studies match well with the open chromatin
137 regions detected by FAIRE.

138 Second, we chose the wing expression of *nubbin* (*nub*) as a case study, and sought to
139 establish a reporter assay system in *Tribolium*. We initially tested the enhancer activity of the
140 open chromatin regions near the *Tribolium nub* locus in *Drosophila*, and identified a region
141 ~40kb upstream of the *Tribolium nub* gene that has wing enhancer activity in *Drosophila*.
142 This region appears to be open uniquely in the wing tissue, thus providing further support for
143 the ability of FAIRE-seq to identify tissue specific enhancers. In parallel, we also identified
144 the wing enhancer of the *Drosophila nub* gene. Then, we made several reporter constructs
145 and tested these constructs in *Tribolium* using the identified *Drosophila* and *Tribolium nub*
146 wing enhancers. We found that the choice of the core promoter is key in establishing a
147 functional reporter assay system in *Tribolium*, and that a construct with the *Drosophila*
148 Synthetic Core Promoter (DSCP) works well in *Tribolium*. This outcome also shows that the
149 region near the *Tribolium nub* locus with wing enhancer activity in *Drosophila* indeed acts as
150 a wing enhancer in *Tribolium*. In addition, using *hunchback* (*hb*) as another example, we
151 demonstrated that our DSCP reporter construct works in other developmental contexts in
152 *Tribolium*.

153 Taken together, our results demonstrate that FAIRE-based chromatin profiling by
154 FAIRE-seq, along with the reporter assay system established in this study, is quite powerful at
155 identifying enhancers, and thus will be useful to study the evolution of *cis*-language in
156 *Tribolium*. In addition, our approach might be applicable in other insects for investigating
157 enhancer function and evolution, which will be advantageous for gaining a more
158 comprehensive understanding of the evolution of *cis*-language.

159

160 **RESULTS**

161 **FAIRE-seq revealed a spatially and temporally regulated chromatin profile in** 162 **the *Tribolium* genome**

163 To obtain chromatin profiles from diverse tissues and stages of *Tribolium*, we performed
164 FAIRE-seq with the following six samples; three stages of embryos (0-24 hours, 24-48 hours,
165 and 48-72 hours), the second (T2) and third thoracic (T3) epidermal tissues of the last instar
166 larvae that contain the forewing (elytron) and hindwing imaginal tissues, and the brain isolated
167 from the last instar larvae. The sequence reads obtained from these FAIRE-seq were then
168 mapped to the *Tribolium* genome assembly (Tcas_3.0). Each sample displays a unique set of
169 open chromatin regions (referred to as “peaks”. See Fig. 2A for example), indicating that the
170 FAIRE-seq with the *Tribolium* tissues was successful. The overall open chromatin
171 characteristics are similar between *Tribolium* and *Drosophila*, however, we also noticed some
172 features unique to the *Tribolium* chromatin profiles. We detected more than 40,000 open
173 chromatin regions in the *Tribolium* genome across the samples (Table 1). To identify
174 differences in open chromatin profiles between samples, we performed differential peak
175 calling using DiffBind (FDR < 0.05). The number of differentially accessible peaks between
176 pairs of samples varied widely. For example, there are over 26,000 differentially accessible
177 peaks between 0-24 hours embryos and T3 (Table 1, Fig. S1), reflecting the extensive
178 differences in *cis*-regulatory control that likely exist between these two samples. By contrast,
179 we found only 4 differentially accessible peaks between T2 and T3. The similarity in open
180 chromatin profiles between T2 and T3 tissues is remarkable given the dramatic differences in
181 morphology between forewing and hindwing in *Tribolium*. However, similar findings were
182 obtained in *Drosophila*, suggesting that both species utilize shared sets of enhancers to shape
183 their appendages. Intriguingly, while the level of nucleosome depletion in the FAIRE-isolated
184 genomic regions is variable between stages and tissues, their positions appear to highly

185 correlate with GC-rich regions of the genome (Fig. S2 A). Furthermore, these
186 GC-rich/FAIRE-identified regions occur with a regular interval, producing a “ruler-like”
187 pattern of FAIRE peaks throughout the genome (Fig. S2 B). This regular periodicity of the
188 GC-rich/FAIRE-identified regions appears to be unique to the *Tribolium* lineage, as we did not
189 detect a similar periodicity in other coleopteran genomes or the genome of a lepidopteran,
190 *Bombyx mori* (Fig. S2 C for *Drosophila*. Data not shown for other insects).

191

192 **Comparison of the FAIRE data to previous enhancer studies in *Tribolium***

193 There are several previous works investigating the activity of *Tribolium* enhancers. To our
194 knowledge, Eckert et al. is the only study analyzing enhancer activity in the *Tribolium* native
195 context, which identified enhancers important for the stripe expression of the *Tribolium hairy*
196 gene (Eckert et al., 2004). Some additional enhancers for *Tribolium* genes have also been
197 identified, albeit in a cross-species context (i.e. *Drosophila*). These include enhancers for
198 *hunchback* (Wolff et al., 1998), *single-minded*, *cactus* and *short gastrulation* (Cande et al.,
199 2009), *labial*, *Dichaete*, and *wingless* (Kazemian et al., 2014). We analyzed the FAIRE profiles
200 at these gene loci and found that FAIRE peaks match with many of the enhancer regions
201 identified through these studies (Fig. S3).

202 More recently, Kazemian et al. applied their enhancer discovery approach, SCRMshaw, to
203 the *Tribolium* genome and predicted 1214 genomic regions as potential enhancers (Kantorovitz
204 et al., 2009; Kazemian et al., 2014). Comparison of the FAIRE data to the SCRMshaw
205 predictions reveals a striking degree of overlap between the two datasets: 78.8% (957/1214)
206 of SCRMshaw predictions overlap at least one embryonic FAIRE peak, while 88.1%
207 (1070/1214) of predictions overlap at least one larval FAIRE peak (Table. S1, S2; $P \approx 0$);
208 overall, 1096 of the 1214 predicted CRMs (90.3%) overlap at least one FAIRE peak. For
209 certain sets of SCRMshaw predictions, the overlaps are even more extensive: for example,

210 98% (97/99) of wing-specific predicted CREs overlap a larval FAIRE peak (Table. S1).
211 Taken together, the high degree of overlap between the FAIRE peaks and previously identified
212 enhancer regions, and FAIRE-peaks and SCRMshaw-predicted CREs, verifies that FAIRE-seq
213 is a powerful tool to identify enhancers in *Tribolium*.

214

215 **Identification of the *Tribolium nub* wing enhancer using an inter-species** 216 **reporter assay**

217 As mentioned in the introduction, reporter assays are a time consuming and laborious task,
218 which makes it difficult to perform in non-*Drosophila* insects, including *Tribolium*. However,
219 to be able to fully exploit the benefit of the FAIRE profiling data, it will be critical to have a
220 reliable method to evaluate the function of *Tribolium* enhancers. The activity of some
221 potential *Tribolium* enhancers has been successfully evaluated via a reporter assay in
222 *Drosophila* (Cande et al., 2009; Kazemian et al., 2014; Wolff et al., 1998; Zinzen et al., 2006).
223 We reasoned that the enhancer of a gene that has a conserved expression pattern (both
224 temporal and spatial) between *Drosophila* and *Tribolium* has the highest chance of being
225 active, even in an inter-species context, and is thus ideal for a case study. The enhancer
226 responsible for the wing expression of *nub* fits this criterion, as *nub* is expressed broadly in
227 the tissues that give rise to wings in both insects (Fig. 1) (Ng et al., 1995; Tomoyasu et al.,
228 2009). In addition, there is an enhancer trap line for *nub* available in *Tribolium* (*pu11*. Fig. 1C,
229 D). We have previously determined that this enhancer trap line has a piggyBac construct
230 inserted about 30kb upstream of the *nub* transcription start site (Clark-Hachtel et al., 2013),
231 which can be used as a starting point to survey for the wing enhancer.

232 *nub* codes for an evolutionarily conserved transcription factor important for the
233 proliferation of wing cells (Ng et al., 1995). *Drosophila* has two *nub* paralogs (*nub* and *pdm2*),
234 while *Tribolium* has one (*Tc-nub*). FAIRE analysis has revealed a number of open chromatin

235 regions located in and near the *Tc-nub* locus (Fig. 2A). Some of the open chromatin regions
236 are shared across the six samples tested (such as the region corresponding to the promoter),
237 but others are unique to specific tissues and stages. We decided to test the two open
238 chromatin regions at or near the *pull* insertion site (*Tc-nub3* and *Tc-nub2*) in *Drosophila* (Fig.
239 2A, B). In addition, we also tested another major open chromatin region located further
240 upstream of the *pull* insertion site (*Tc-nub1*). This region is open predominantly in the larval
241 T2 and T3 epidermal tissues (containing the future wing tissues) but not in any of the
242 embryonic samples, suggesting the possibility that this region contains enhancers specific to
243 the post-embryonic stage (Fig. 2A, B).

244 The inter-species reporter assay showed that *Tc-nub2* and *Tc-nub3* do not have
245 enhancer activity in the future wing-related tissues (wing and haltere imaginal discs) when
246 tested in *Drosophila* (Fig. 2C-F). *Tc-nub3* showed activity in a small region near the hinge of
247 the wing and haltere disc, but not in the region that gives rise to the wings (wing and haltere
248 pouches) (Fig. 2C, D). *Tc-nub2* drove the reporter expression in the leg discs, but did not
249 show any enhancer activity in the wing and haltere discs (Fig. 2E, F). In contrast, *Tc-nub1*
250 showed significant enhancer activity in the pouch region of the wing disc (Fig. 2G). *Tc-nub1*
251 also drove reporter expression in the leg disc, but was not active in the haltere disc (Fig. 2H).
252 Since *Tc-nub1* corresponds to the region uniquely open in the larval epidermis in *Tribolium*,
253 the outcome of our inter-species reporter assay indicates that (i) the open chromatin profiling
254 of various tissues and stages by FAIRE-seq in *Tribolium* can help predict tissue/stage specific
255 enhancers from the *Tribolium* genome, and (ii) the inter-species reporter assay can be useful,
256 at least for the enhancers responsible for the post-embryonic expression of *nub* in *Tribolium*.

257 We next sought to minimize the *Tc-nub* wing enhancer by testing three shorter
258 fragments within the *Tc-nub1* region (Fig. 2B). Interestingly, despite covering the main
259 FAIRE peak region of *Tc-nub1*, *Tc-nub1Core* did not show any enhancer activity in the wing

260 (Fig. 2K, L). Instead, *Tc-nub1L*, which corresponds to only a part of the major open
261 chromatin region, drove the reporter expression with a pattern and level almost identical to
262 *Tc-nub1* (Fig. 2I, J). *Tc-nub1R* did not show any enhancer activity (Fig. 2M, N). These results
263 suggest that the important elements for driving wing expression reside within the first 200bp
264 of *Tc-nub1*. We tested this idea by making a reporter construct using only the 200bp region
265 unique to *Tc-nub1L* (*Tc-nub1La*, Fig. 2B). This fragment drove the reporter expression in the
266 wing and leg discs, albeit with a more restricted expression domain and/or a lower expression
267 level compared to *Tc-nub1L* (Fig. 2O, P). We also tested a construct that contains the
268 *Tc-nub1L* region along with an additional 200bp sequence outside of *Tc-nub1* (*Tc-nub1Lb* in
269 Fig. 2B), since the location of the functional *Tc-nub* wing enhancer may be slightly
270 misaligned with the open chromatin region predicted by FAIRE. However, *Tc-nub1Lb*
271 showed even weaker enhancer activity (Fig. 2Q, R), suggesting that there might be a
272 suppressor element next to the *Tc-nub1* region. The constructs we made also drove reporter
273 expression outside of the wing and leg imaginal disc. These results are summarized in Table
274 S3.

275

276 **Identification of the *Drosophila nub* wing enhancer using a combination of**
277 **genomic resources, FAIRE profiling, and the reporter assay approach in**
278 ***Drosophila***

279 As a comparison to the enhancer identified via an inter-species reporter assay
280 described above, we sought to identify the *nub* wing enhancer native to the species used for
281 the reporter assay (i.e. *Drosophila*). As mentioned, there are two *nub* paralogs in *Drosophila*
282 (*nub* and *pdm2*), both of which have similar expression in the wing pouch (Ng et al., 1995).
283 We first took advantage of the FlyLight project and surveyed the *nub* and *pdm2* loci for a
284 genomic region that has wing enhancer activity. Among the 33 constructs tested in FlyLight

285 (Fig. 3A), one region (GMR11F02) has a record of enhancer activity in the wing and haltere
286 pouch, along with additional expression in the leg disc (Fig. 3B, C). We then utilized the
287 previously published FAIRE profile for *Drosophila* (McKay and Lieb, 2013), and identified
288 three distinct regions within GMR11F02 that are open in the wing and haltere discs (Fig. 3A).
289 We cloned these three regions (Fig. 3B, *Dm-nub1*, *Dm-nub2*, and *Dm-nub3*), and tested their
290 enhancer activity in *Drosophila*. Among the three regions, *Dm-nub2* displayed strong
291 enhancer activity in the wing pouch region (Fig. 3G, H). *Dm-nub1* (Fig3E, F) and *Dm-nub3*
292 (Fig3I, J) did not drive reporter expression in the wing and haltere discs. In addition,
293 *Dm-nub3* was active in the leg disc, suggesting that the *nub* wing/haltere enhancer and the leg
294 enhancer are separable (Fig. 3J). To further minimize the *Dm-nub* wing enhancer, we tested
295 three shorter fragments within *Dm-nub2* (*Dm-nub2a*, *Dm-nub2b*, and *Dm-nub2c*. Fig. 3D).
296 The wing related expression is driven by *Dm-nub2a*, albeit at a weaker level (Fig. 3K, L).
297 This suggests that, although *Dm-nub2a* contains sufficient components to drive wing
298 expression, a broader genomic region is required for robust wing expression of *Dm-nub*. In
299 contrast, *Dm-nub2b* and *Dm-nub2c* did not drive any expression (Fig. 3M-P). The expression
300 patterns of these constructs in other tissues are summarized in Table S4. Taken together, the
301 *Dm-nub2* region we isolated (1.3kb) is sufficient to drive a robust wing expression in
302 *Drosophila*.

303

304 **Establishing a reporter assay system and evaluating the *nub* wing enhancers in** 305 ***Tribolium***

306 Although some *Tribolium* enhancers were shown to be active in the cross-species context,
307 these enhancers still need to be examined in their native species for functional validation.
308 However, the lack of a reliable reporter construct has been a major obstacle in performing
309 functional evaluation of enhancers in *Tribolium*. The GATEWAY system (Katzen, 2007) has

310 been useful in quickly cloning genomic regions into a reporter construct and testing their
311 enhancer activity in *Drosophila*. We sought to establish a GATEWAY compatible reporter
312 construct that is functional in *Tribolium*.

313 A key issue in establishing a reporter construct is the choice of promoters. Previous
314 studies have raised concerns about using *Drosophila* promoters in *Tribolium* (Schinko et al.,
315 2010). While establishing the Gal4/UAS system in *Tribolium*, Schinko et al. found that the
316 core promoter isolated from a *Tribolium* endogenous gene, *Tc-hsp68*, worked more efficiently
317 when compared to the exogenous promoters that were tested (Schinko et al., 2010). We
318 therefore made a GATEWAY compatible piggyBac construct that contains the *Tc-hsp68* core
319 promoter driving the *dsRed* gene (piggyGHR, Fig. 4A). In addition, we added the *gypsy*
320 element, a *Drosophila* insulator, flanking the reporter assay construct to prevent position
321 effects (Fig. 4A). We tested this piggyBac construct with the *Tribolium* and *Drosophila nub*
322 wing enhancers (*Tc-nub1L* and *Dm-nub2*) in *Drosophila*. Both *Tc-nub1L* and *Dm-nub2* drove
323 dsRed expression identical to the patterns obtained with the *Drosophila* reporter construct
324 (compare Fig. 4B, C to Fig. 2I, J, and Fig. 4D, E to Fig. 3G, H), confirming that piggyGHR is
325 functional. However, neither *Tc-nub1L* or *Dm-nub2* in piggyGHR showed consistent
326 enhancer activity in the wing tissues when transformed into *Tribolium* (Fig. 4F-M). Among
327 the seven independent transgenic lines obtained for piggyGHR-*Tc-nub1L*, none of them had
328 clear dsRed expression in the wing tissues (Fig. 4F-K). Instead, four lines had dsRed
329 expression in non-wing tissues, with a distinct pattern in each line, likely due to trapping
330 local enhancers (Fig. 4F-K). We obtained only two independent transgenic lines for
331 piggyGHR-*Dm-nub2*, neither of which had dsRed expression in the wing tissue (Fig. 4L, M).
332 These results indicate that our construct with the *Tc-hsp68* core promoter does not work well
333 for reporter assays, at least in the wing related tissues in *Tribolium*, although it does work in
334 *Drosophila*. Alternatively, it is also possible that the *Drosophila gypsy* insulators we added to

335 the construct might not be functioning properly in *Tribolium*.

336 We next tested a synthetic promoter in *Tribolium*. Pfeiffer et al. modified the Super
337 Core Promoter 1 (SCP1) (Juven-Gershon et al., 2006) and constructed the *Drosophila*
338 Synthetic Core Promoter (DSCP), which was used for the FlyLight project as well as other
339 *Drosophila* reporter constructs including pFUGG used in this study (McKay and Lieb, 2013).
340 We made a piggyBac construct with the DSCP driving mCherry (piggyGUM, Fig. 5A). We
341 decided to remove the *Drosophila gypsy* insulators from our construct to avoid possible
342 inter-species issues. Similar to piggyGHR, piggyGUM with the *Drosophila* and *Tribolium*
343 *nub* wing enhancers drove reporter expression in the wing disc in *Drosophila* (Fig. 5B-E),
344 confirming that piggyGUM is functional. In *Tribolium*, in contrast to the piggyGHR
345 constructs, piggyGUM-*Tc-nub1L* successfully recaptured the expression pattern of the *nub*
346 enhancer trap line (*pull*) and drove reporter expression in the wing related tissues (both in T2
347 and T3) at both larval and pupal stages (Fig. 5F-I, compared to Fig. 1C, D).
348 piggyGUM-*Dm-nub2* also showed enhancer activity in the larval wing discs in *Tribolium*
349 (Fig. 5J-L). The expression driven by *Dm-nub2* in *Tribolium* was mostly in the wing hinge
350 and the margin regions, similar to the pattern observed for this enhancer in the *Drosophila*
351 imaginal discs (Fig. 3G, H, Fig. 5D, E). These results indicate that (i) our GATEWAY
352 compatible DSCP piggyBac construct (piggyGUM) can be used for reporter assays both in
353 *Tribolium* and *Drosophila*, and (ii) the *Tribolium nub* wing enhancer identified through an
354 inter-species reporter assay (*Tc-nub1L*) is indeed functional as a wing enhancer in *Tribolium*.
355 It is also worth mentioning that some of the piggyGUM transgenic lines showed mCherry
356 expression in tissues outside of wings (data not shown). The expression patterns outside of
357 the wing related tissues were not consistent among the transgenic lines, suggesting that the
358 piggyGUM construct also occasionally traps endogenous enhancers.

359 We also tested if the promoter endogenous to the enhancer works better for a reporter

360 assay construct in *Tribolium*. We made a piggyBac construct with the 2kb sequence upstream
361 of the *Tc-nub* transcription start site (confirmed by 5' RACE (Clark-Hachtel et al., 2013)) as
362 the promoter (Fig. 6A, piggyNub-proR). We also used the 2kb downstream of the *Tc-nub* stop
363 codon (confirmed by 3' RACE (Clark-Hachtel et al., 2013)) as the 3' untranslated region
364 (UTR) and the poly A signal native to *Tc-nub* (Fig. 6A). We made a similar construct for
365 Tc-Act5c (1kb upstream of the transcription start site and 1kb downstream of the stop codon
366 as the native promoter and polyA signal, respectively) as a comparison (Fig. 6B). To our
367 surprise, *Tc-nub1L* in piggyNub-proR did not drive any expression in *Tribolium* (Fig. 6C-F)
368 or in *Drosophila* (Fig. 6G, H). Realtime-qPCR analysis revealed that there is no transcription
369 of dsRed in these transgenic lines in both species (data not shown), suggesting that the lack of
370 reporter expression is not due to incompatibility of the reporter gene with the *Tc-nub* UTRs
371 and is rather due to the *nub* wing enhancer failing to work with the endogenous promoter
372 and/or polyA signal. In contrast to piggyNub-proR- *Tc-nub1L*, piggyAct5cR shows strong
373 and ubiquitous dsRed expression in *Tribolium* (Fig. 6I), indicating that our strategy of
374 incorporating the endogenous transcription and translation components is valid. Intriguingly,
375 however, piggyAct5cR did not drive any expression in *Drosophila* (data not shown),
376 implying a strict species specific nature of the transcription and/or translation components
377 (such as promoters), even for an evolutionarily highly conserved house-keeping gene that is
378 uniformly expressed in various species including *Drosophila* and *Tribolium* (Chung and
379 Keller, 1990).

380

381 **Testing the reporter construct in another context in *Tribolium***

382 We next wondered if our DSCP reporter system works in a context other than wings in
383 *Tribolium*. We chose *hb* as a case study, and tested the reporter activity during embryogenesis.
384 *hb* expression in *Tribolium* starts as a broad posterior domain in the blastoderm and clears

385 from posterior to form an anterior band of expression that covers pre-gnathal and gnathal
386 segments (Lynch et al., 2012; Marques-Souza et al., 2008). In the early germband stage, the
387 band resolves into a stripe covering the labium (Fig. 7B) (Marques-Souza, 2007; Zhu et al.,
388 2017). Wolff et al. previously identified a genomic region at the *Tribolium hb* locus that
389 drives blastoderm expression when introduced in *Drosophila* (Fig. 7A, orange bar) (Wolff et
390 al., 1998). This region corresponds to a SCRMshaw prediction (Fig. 7A, purple bars).
391 Therefore, although the FAIRE signal at this region is weak (likely due to the wide time
392 window of sampling during early embryogenesis), the outcomes of previous studies make
393 this region an excellent candidate enhancer to test with our reporter system in *Tribolium*. We
394 cloned a 1340bp fragment containing this genomic region (*hb*-PE1, Fig. 7A, red bar), and
395 tested its enhancer activity using the piggyGUM construct in *Tribolium*. *in situ* hybridization
396 for the *mCherry* reporter gene revealed that the piggyGUM-PE1 construct recapitulates the
397 *hb* expression at the early germband stage in *Tribolium* (Fig. 7C). This result indicates that (i)
398 our DSCP reporter system works well even during embryogenesis in *Tribolium*, and (ii)
399 *hb*-PE1 contains the *hb* early germband enhancer.

400 In summary, we established a functional reporter assay system that works in diverse
401 developmental contexts in *Tribolium* and also successfully identified the enhancers
402 responsible for wing expression of *nub* and early germband expression of *hb*. Furthermore,
403 our reporter construct (piggyGUM) is compatible in both *Drosophila* and *Tribolium*,
404 implying that this reporter construct may be applicable even to other insect species.

405 **DISCUSSION**

406 In this study, we demonstrated that FAIRE-based chromatin profiling is a powerful approach
407 for identifying CREs, such as enhancers, in *Tribolium*. The *Tribolium nub* wing enhancer we
408 identified (*Tc-nub1L*) is over 40kb away from the *nub* transcription start site, and 10kb away
409 from the *pull* insertion site, which would be very difficult to identify without the aid of open
410 chromatin profiles. In addition, with the usage of the DSCP, we were able to establish a
411 functional reporter assay construct in *Tribolium*. Combination of FAIRE-based chromatin
412 profiling with this reporter assay system will allow us to assess the function and evolution of
413 enhancers in *Tribolium*.

414

415 **FAIRE profiles in *Tribolium***

416 Genome-wide FAIRE profiling in *Tribolium* has identified a significant number of genomic
417 regions whose chromatin status is regulated in a tissue and stage specific manner (Table 1, Fig.
418 S1). These regions are promising candidates for future enhancer studies in *Tribolium*. In
419 addition, our FAIRE analysis has revealed both evolutionarily conserved and diverged aspects
420 of chromatin state regulation between *Drosophila* and *Tribolium*. For the conserved aspect, we
421 saw similar chromatin profiles for the T2 and T3 epidermal samples, even though these two
422 tissues differentiate into morphologically distinct structures (the elytron in T2 and hindwing in
423 T3). This outcome echoes the message obtained from the *Drosophila* FAIRE study, namely
424 that chromatin profiles are largely similar among the similar lineages of tissues (such as legs,
425 wings, and halteres), with the exception of a handful of “master control gene” loci (McKay and
426 Lieb, 2013). In fact, three of the four differentially-open FAIRE peaks between T2 and T3 in
427 our *Tribolium* FAIRE analysis are within the *Ultrabithorax* (the T3 selector gene) locus (Fig.
428 S1) (to review the function of *Ultrabithorax* during wing development, see (Tomoyasu, 2017)).
429 In contrast, the *Tribolium* FAIRE profiles during embryogenesis show an interesting difference

430 when compared to those in *Drosophila*. In *Drosophila*, the number of genomic regions that are
431 open is fairly consistent throughout embryogenesis, with a distinct set of genomic regions
432 being open in each stage (McKay and Lieb, 2013). In *Tribolium*, we noticed that a larger
433 number of chromatin regions are open early in embryogenesis, and some of these regions are
434 subsequently closed, resulting in a smaller number of open chromatin regions in later stages.
435 This difference may be a reflection of the different modes of embryogenesis found in the two
436 insects (long vs. short germ band embryogenesis), although the significance of the difference
437 in chromatin profiles is yet to be investigated.

438 We also noticed a strict overlap between the GC-rich regions and FAIRE-detected open
439 chromatin regions. This raises an interesting argument about the evolution of enhancers. Are
440 these regions open because they are functionally important (such as enhancers)? Or, have these
441 regions become enhancers, because they were open due to a bias in their nucleotide content and
442 thus accessible to transcription factors? There appears to be a similar correlation among the
443 GC-rich regions, enhancers, and FAIRE peaks in *Drosophila* (Li et al., 2007; McKay and Lieb,
444 2013). It will be interesting to investigate how GC-rich regions overlap with open chromatin
445 regions in other insects. In addition, we found that the GC-rich/FAIRE-positive regions appear
446 in a regular interval throughout the *Tribolium* genome. The molecular basis and functional
447 implication of this periodicity is currently unknown, however, it is intriguing to speculate that a
448 genome-wide event (such as transposon invasion) might have significantly influenced the
449 chromatin state landscape in the *Tribolium* lineage.

450

451 **Overlaps between FAIRE and SCRMshaw enhancer prediction**

452 The high degree of overlap observed between FAIRE peaks and enhancers predicted by the
453 completely different, solely computational, SCRMshaw method provides further
454 confirmation that FAIRE is an effective means for enhancer discovery in *Tribolium*. Overall,

455 the number of FAIRE peaks is well in excess of the number of SCRMshaw predictions.
456 Several factors likely account for this result. First, the SCRMshaw predictions were
457 performed at high stringency in order to minimize potential false-positive results (Kazemian
458 et al., 2014); relaxing the prediction criteria would yield more predicted enhancers. While this
459 would potentially lead to more false positives, the >90% overlap seen for several specific
460 data sets (Table S1) suggests that stringency could be relaxed in at least some cases. Second,
461 SCRMshaw relies on training data from known *Drosophila* enhancers; therefore enhancers
462 with properties significantly deviating from those of *Drosophila* enhancers will be found only
463 by chromatin profiling, such as FAIRE. Finally, although FAIRE appears to be biased toward
464 enhancers (Song et al., 2011), it also identifies other regions of open chromatin such as
465 promoters and insulator regions (Giresi et al., 2007), which are not predicted by the
466 enhancer-specific SCRMshaw.

467 The twin issues of higher SCRMshaw false-positive rates at lower prediction
468 stringencies and FAIRE's lack of discrimination with respect to enhancers with specific
469 spatial and temporal activity profiles suggest that considerable advantages could be obtained
470 by using the methods in combination. Overlap with FAIRE peaks can be used to filter out
471 false-positive SCRMshaw predictions, allowing predictions to be performed at lower
472 stringency and thus higher sensitivity. Conversely, SCRMshaw prediction can be used to
473 focus on potentially more relevant FAIRE peaks, helping to avoid selecting sequences
474 representing enhancers active in tissues other than the one of interest; enhancers for a
475 neighboring housekeeping gene; insulators; and cryptic promoters or those for unannotated
476 genes. This will be particularly useful for situations like the one seen here for the larval
477 samples, where cleanly separating wing from body wall tissue was difficult, a common
478 challenge when attempting to isolate tissues from small organisms such as insect embryos.
479

480 **Enhancer activity in inter-species contexts and the limitation of non-native**
481 **reporter assays**

482 Our reporter assays in two insect species showed that both *Drosophila* and *Tribolium nub*
483 wing enhancers were at least partially active in the inter-species context. We identified a
484 20-bp sequence shared between the two enhancers that contains binding sites of some
485 wing-related transcription factors (such as Brinker and Mad) (Fig. S4). However, deletion of
486 this sequence did not influence the activity of these enhancers when tested in *Drosophila*,
487 indicating that this sequence is dispensable for enhancer function (Fig. S4). We did not
488 recognize any other significant sequence similarity or a conserved TF-binding site
489 architecture between the two enhancers, suggesting that the regulatory landscape in the wing
490 of the two species is evolutionarily maintained (as the *nub* enhancers can be functional in
491 inter-species contexts) despite the lack of noticeable sequence conservation in the enhancer
492 itself. A thorough examination of *trans* properties that regulate the *nub* wing enhancers may
493 give us insights into how enhancers evolve under a conserved regulatory landscape.

494 Although the *Tribolium* wing enhancer was active in *Drosophila*, we noticed that the
495 activity of this enhancer was somewhat restricted, as it was active mainly at the dorsal-ventral
496 (DV) compartmental boundary of the T2 wing, and only in a few cells in the haltere. This is
497 in contrast with the expression in *Tribolium*, which showed a broader activity domain in the
498 entire wing tissues both in the T2 and T3 segments. These differences in the activity domains
499 suggest that some components that regulate the *Tribolium nub* wing enhancer are missing
500 from the *Drosophila* T2 wing and almost entirely absent in the haltere. This highlights the
501 limitation of inter-species analyses and the importance of performing reporter assays in the
502 native species. The reporter assay system we developed now allows us to analyze enhancer
503 activities in *Tribolium*. The successful demonstration of reporter analyses for *nub* in the wing
504 and *hb* in the embryo suggest that our reporter construct works in various tissues; however, it

505 is still crucial to evaluate the applicability of this system in diverse contexts.

506

507 **Choice of core promoters in reporter constructs**

508 Our study showed that the choice of promoters is critical when assessing enhancer activity.

509 *Tc-hsp68* was our first choice because it has successfully been used in the Gal4/UAS system

510 in *Tribolium* (Schinko et al., 2010). However, in our reporter assay, although this promoter

511 worked efficiently in *Drosophila*, it failed to drive reporter expression even with a functional

512 enhancer in *Tribolium* (at least in our hands). Interestingly, the transgenic beetles with the

513 *Tc-hsp68* reporter construct showed high occurrence of enhancer trap events (Fig. 4F-M),

514 even though this promoter failed to work with the enhancer we placed right upstream of it.

515 One explanation is that this promoter requires a certain distance for optimal interaction with

516 enhancers in *Tribolium*. The situation might be less strict in *Drosophila* (for an unknown

517 reason), allowing the *Tc-hsp68* promoter to overcome the distance requirement.

518 We also tried to assess the *nub* wing enhancer activity with the *nub* endogenous

519 promoter, but to our surprise, this construct did not drive any expression. There are several

520 possible explanations for this outcome. First, the region we selected might not contain the

521 correct promoter for the *nub* transcript, although our 5' RACE results (as well as the

522 published *Tribolium* genome annotation (Tribolium Genome Sequencing et al., 2008))

523 supports our annotation of the *nub* transcription start site (Clark-Hachtel et al., 2013). Second,

524 the 2kb region we used as the promoter may contain a suppressor element, interfering with

525 the enhancer to drive reporter expression. Third, the *nub* promoter might require a long

526 distance to interact properly with the wing enhancer, as the wing enhancer we identified is

527 40kb away from the *nub* transcription start site. This might parallel the situation with

528 *Tc-hsp68*, in which this promoter preferably works with enhancers located at a certain

529 distance. This may further support the idea that *Drosophila* are more permissive to changes in

530 the enhancer/promoter distance. However, in the case of the *nub* endogenous promoter, there
531 might be additional issues other than enhancer/promoter distance that prevented this reporter
532 construct from working even in *Drosophila*.

533 The reporter construct with the DSCP (piggyGUM) worked efficiently both in
534 *Drosophila* and *Tribolium*. The DCSP is a synthetic core promoter, composed of several
535 common core promoter motifs (i.e. TATA box, Inr, MTE, and DPE) isolated from the
536 *Drosophila* genome. The DSCP has been shown to work efficiently with a diverse array of
537 developmental enhancers in various contexts in *Drosophila* (Pfeiffer et al., 2008; Zabidi et al.,
538 2015), suggesting that this promoter may also work well with other enhancers in *Tribolium*.
539 However, it is worth mentioning that a synthetic promoter similar to the DCSP, SCP1
540 (composed of *Drosophila* and viral promoter motifs (Juven-Gershon et al., 2006)), failed to
541 work when tested in the Gal4/UAS system in *Tribolium* (Schinko et al., 2010). This again
542 emphasizes the importance of choosing the correct promoter that fits the context of the study,
543 which remains a critical area for further exploration.

544

545 **Enhancer studies in evo-devo**

546 The study of enhancers and other CREs is critical to understand the molecular basis
547 underlying morphological evolution, as changes in gene regulation, rather than the
548 acquisition of new genes or the modification of protein structures, are often responsible for
549 the evolution of the diverse array of morphology (Carroll, 2008). For example, changes in
550 enhancers can facilitate evolution of novel structures via co-opting preexisting GRNs into a
551 new context. Acquisition of enhancers *de novo* may also play a critical role in morphological
552 novelty. Therefore, studying both evolutionarily conserved and diverged enhancers will help
553 further our understanding of morphological evolution (see (Monteiro and Podlaha, 2009) for
554 a comprehensive discussion of how *cis* studies can help elucidate the molecular basis for the

555 evolution of novel traits) . However, it has been a challenge to study enhancers in
556 non-traditional model insects due to the lack of a reliable enhancer identification strategy. In
557 this study, we showed that FAIRE-seq is readily applicable to non-traditional model species.
558 Furthermore, the DSCP can be a useful promoter for establishing a reporter assay system and
559 investigating the evolution of enhancers in non-*Drosophila* insects. Therefore, FAIRE-based
560 chromatin profiling, along with reporter assay systems applicable to various insects, will
561 make the research on enhancers more accessible, which will provide us with more insights
562 into the evolution of the regulatory mechanisms underlying morphological diversity.
563

564 MATERIALS AND METHODS

565 Fly stocks

566 The following two *Drosophila* strains used in this study were obtained from the Bloomington
567 *Drosophila* Stock center.

568 $P\{UAS-Dcr-2.D\}^l, w^{1118}; P\{GawB\} nubbin-AC-62$

569 $y^l w^*; wg^{Sp-1}/CyO, P\{Wee-P.ph0\}Bacc^{Wee-P20}; P\{20XUAS-6XGFP\}attP2.$

570

571 Beetle cultures

572 The beetle cultures were reared on whole wheat flour (+5% yeast) at 30 °C in a temperature and
573 humidity controlled incubator. The *nub* enhancer trap line *pull1*, which has enhanced yellow
574 fluorescent protein (EYFP) expression in the hindwing and elytron discs (Clark-Hachtel et al.,
575 2013; Lorenzen et al., 2003; Tomoyasu et al., 2005), was used as to monitor *nub* expression in
576 *Tribolium*.

577

578 Tissue preparation for FAIRE

579 For the *Tribolium* larval T2 and T3 wing tissues, the dorso-lateral portion of the epidermal
580 tissues that contain elytron (T2) and hindwing (T3) discs were dissected from the last instar
581 larvae. Although these samples largely consisted of tissues that give rise to wing structures,
582 they also contained body wall tissues as well as larval muscles due to difficulty of precisely
583 dissecting the wing tissues from larvae. About 50 larvae (100 dissected tissues) were used for
584 each biological replicate, with three replicates prepared for each wing sample. The brains
585 were dissected from the head of the last instar larvae. About 40 brains were used for each
586 biological replicate, with two replicates prepared. Embryos were collected in whole wheat
587 flour (+5% yeast) for 24 hours at 30 °C. The collected embryos were cultured for one and two
588 days at 30 °C for the 24-48 hour and 48-72 hour samples, respectively. 0.1g of embryos were

589 used for each biological replicate, with three replicates prepared for each sample. These
590 tissues and embryos were crosslinked with 4% formaldehyde for 30 min (larval tissues) or
591 8% formaldehyde for 30 min (embryos).

592

593 **FAIRE-seq analysis**

594 FAIRE was performed as previously described (McKay and Lieb, 2013). FAIRE-seq libraries
595 were sequenced on an Illumina HiSeq 2000 at the University of North Carolina
596 High-Throughput Sequencing Facility. 50bp single-end Illumina reads were obtained for
597 FAIRE-treated samples and two non-FAIRE-treated input samples. Reads were trimmed to
598 remove index sequence and mapped to the *Tribolium* reference genome (version 3.0) with
599 bowtie2 (Langmead and Salzberg, 2012). Read alignments were quality filtered (Q<10
600 dropped) and duplicate reads were removed using SAMtools. For visualization of FAIRE
601 signal, bigwig files were produced by merging tissue/stage-specific replicate bam files with
602 SAMtools and normalizing reads to sequencing depth using deepTools. These files were then
603 visualized with the IGV genome viewer (Robinson et al., 2011; Thorvaldsdóttir et al., 2013).
604 Peaks were called on individual replicates using MACS2 with the merged input sample bam
605 files as the control. The *Drosophila* FAIRE profiles used in this study were previously
606 published (McKay and Lieb, 2013). For differentially open peak analysis, mapped reads (.bam
607 files) for each replicate and the merged input, along with MACS2 peaks (.narrowPeak files)
608 called for each replicate, were provided as input for DiffBind. DiffBind creates a consensus
609 peakset for all replicates provided, requiring a consensus peak to be present in at least 2
610 replicates of 1 sample. An experiment-wide consensus peakset was produced using all samples.
611 Pairwise analysis of differentially open peaks between samples was performed within DiffBind
612 with the DESeq2 method for all consensus peaksets, and plotted using the `dba.plotMA()`
613 function. The differentially open peaks are listed in Table S6.

614

615 **Genome-wide GC-contents analysis**

616 Using the experiment-wide consensus peakset described above, 1 kb of sequence upstream and
617 downstream of each peak center was extracted from the genome using BEDTools (Quinlan and
618 Hall, 2010) and custom Python scripts. For these 2kb fragments, those free of Ns were
619 subjected to GC analysis. Changes in local GC content (250bp sliding window, 10bp step)
620 were plotted against the whole-fragment average of GC content for all fragments. For the
621 GC-rich region distance analysis, first, bedGraphs of GC content fluctuations above and below
622 the genome wide average were computed at 70 and 60bp resolution for the *Tribolium* and
623 *Drosophila* genomes, respectively. The genome of *Bombyx mori*, as well as the genomes of
624 several coleopteran insects (*Agrilus planipennis*, *Dendroctonus ponderosae*, *Anoplophora*
625 *glabripennis*, *Leptinotarsa decemlineata*, *Nicrophorus vespilloides*, and *Onthophagus taurus*)
626 were analyzed at 70bp resolution. Peaks were then called using the bdgcallpeak command in
627 MACS2. Distance between the edges of adjacent peaks was categorized into 100bp bins and
628 the ln of the number of occurrences plotted. For the FAIRE peak distance analysis, distances
629 between FAIRE peaks were collected and plotted in the same manner as the GC peaks. A
630 consensus *Drosophila* FAIRE peakset was obtained from DiffBind with the same settings as
631 the *Tribolium* data using the previously published data (McKay and Lieb, 2013).

632

633 **Comparison between FAIRE and SCRMshaw**

634 Enhancers predicted by SCRMshaw were taken from Table S4 of Kazemian et al. (Kazemian
635 et al., 2014) and converted into BED format. BEDTools *merge* was used to combine
636 overlapping and/or redundant (i.e., from more than one SCRMshaw scoring method)
637 predictions, reducing the total number of predicted enhancers to 1214. BEDTools *intersect*
638 was then used to determine all predicted enhancers with at least 50 bp overlap with a FAIRE

639 peak (-f 0.10). FAIRE peaks not assigned to a *Tribolium* chromosome (i.e., not starting with
640 “ChLG”) were omitted. Significance of overlaps was determined using BEDTools *fisher*; all
641 overlaps were highly significant with $-\log(P) \geq 19$. Because this method provides only an
642 approximation, a selection of datasets was tested via randomization. BEDTools *shuffle* was
643 used to generate 1000 random intervals and the intersections were determined as above. The
644 mean and standard deviation of the randomized intersections were calculated and used with
645 the observed (SCRMshaw) intersection value to determine a *z* score. *P* values from all
646 randomization tests were highly significant.

647

648 ***Drosophila* reporter assay constructs**

649 pFUGG, a *Drosophila* GATEWAY-compatible phiC31 transformation plasmid, was used for
650 reporter assay in *Drosophila* (McKay and Lieb, 2013). The phiC31 system allows site-specific
651 integration (Bischof et al., 2007), thus preventing position effects due to different insertion
652 sites. An enhancer cloned into pFUGG will drive Gal4 as the reporter, whose expression
653 domains will then be visualized by crossing to UAS-EGFP flies.

654

655 **GATEWAY compatible piggyBac reporter constructs**

656 The piggyBac plasmid with the 3xP3-EGFP marker construct and the FseI/AscI cloning site
657 (Horn and Wimmer, 2000) was used to make all piggyBac constructs used in this study. For
658 **piggyGHR** (piggyBac GATEWAY Tc-hsp68 dsRed), the *gypsy* element, *Tc-hsp68* core
659 promoter, *dsRed*, and the SV40 polyA signal were amplified by PCR, assembled through
660 ligation, and inserted into the FseI/AscI site of the piggyBac plasmid. The assembled plasmid
661 was then converted to a GATEWAY compatible plasmid by Gateway® Vector Conversion
662 System (ThermoFisher Science). For **piggyGUM** (piggyBac GATEWAY Universal promoter
663 mCherry), the reporter construct including the GATEWAY cassette was amplified from a

664 *Drosophila* GATEWAY-compatible phiC31 transformation vector and inserted into the
665 FseI/AscI site of the piggyBac plasmid. The primers used to make piggyGUM were listed in
666 Table S5. The reporter constructs in **piggyNub-proR** (*piggyBac nub* promoter dsRed) and
667 **piggyAct5c-proR** (*piggyBac Act5c* promoter dsRed) were *de novo* synthesized and inserted
668 into the FseI/AscI site of the piggyBac plasmid.

669

670 **Enhancer cloning**

671 Genomic fragments corresponding to possible enhancer regions were PCR amplified and
672 cloned into pENTR using pENTR-D Directional TOPO Cloning kit (Thermo-Fisher
673 Scientific, K240020). The primers used to clone the enhancer regions from the *Drosophila*
674 and *Tribolium* genome are listed in Table S5. Cloned genomic fragments were then inserted
675 into reporter constructs via GATEWAY Clonase reaction (Thermo-Fisher Scientific,
676 11791-019).

677

678 ***Drosophila* and *Tribolium* transgenesis**

679 For *Drosophila* transgenesis, pFUGG constructs were transformed into the attP2 site (68A4)
680 through PhiC31 integrase-mediated transgenesis system, and piggyBac constructs were
681 transformed into *w¹¹¹⁸* with EGFP as a visible marker (BestGene *Drosophila* transgenic
682 service). For *Tribolium* transgenesis, piggyBac constructs were transformed into
683 *vermilion^{white}* with EGFP as a visible marker (TriGenES *Tribolium* Genome Editing Service
684 for the *nub* and *Act5c* constructs, Friedrich-Alexander-Universität Erlangen-Nürnberg for the
685 *hb* construct).

686

687 **Immunohistochemistry and *in situ* hybridization**

688 *Drosophila* imaginal discs were dissected from the third instar larvae and fixed with 4%

689 formaldehyde for 25 min. *Tribolium* elytron and hindwing discs were dissected from the last
690 instar larvae, and fixed with 4% formaldehyde for 25 min. Dissected tissues were then
691 washed and blocked with 10% BSA, and incubated with Rabbit anti-mCherry antibody
692 (1:500; Abcam, ab167453) at 4 °C for overnight. After washing for one hour, the tissues were
693 incubated with the Alexa 555 conjugated Goat anti-Rabbit antibody (1:500) for 2 hours at
694 room temperature. All the discs were mounted on glass slides with ProLong® Gold antifade
695 reagent (Life Technologies) for documentation. *in situ* hybridization was performed as
696 previously described (Shippy et al., 2009), with DIG-labeled riboprobes and alkaline
697 phosphatase conjugated anti-DIG antibody (Sigma-Aldrich 11093274910). Signal was
698 developed using BM Purple (Sigma-Aldrich 11442074001). The primers used to amplify the
699 *mCherry* fragment for riboprobe synthesis were included in Table S5. The *hb* riboprobe used in
700 this study is previously described (Wolff et al., 1998).

701

702 **Image Processing and Documentation**

703 The images were captured by Zeiss 710 confocal microscope (mounted discs) and Zeiss
704 AxioCam MRc5 with Zeiss Discovery V12 (*Tribolium* larvae and pupae). A filter set specific
705 to mCherry (575/50x, 640/50m) was used to visualize the mCherry expression driven by
706 piggyGUM constructs. *Tribolium* germband embryos were imaged with ProgRes CFcool
707 camera on Zeiss Axio Scope.A1 microscope using ProgRes CapturePro image acquisition
708 software. Some pictures were enhanced only for brightness and contrast with Adobe
709 Photoshop.

710

711 **Acknowledgements**

712 We thank the Bloomington Stock Center for fly stocks, and the Center for Bioinformatics and Functional
713 Genomics (CBFG) and Center for Advanced Microscopy and Imaging (CAMI) at Miami University for
714 technical support. We also thank Shuxia Yi for technical support, and Courtney Clark-Hachtel, David Linz, and
715 other members of Tomoyasu lab for helpful discussion.

716

717 **Competing interests**

718 The authors declare no competing or financial interests.

719

720 **Author contributions**

721 Y.T. designed the project. Y-T.L., K.D.D., F.B-C., N.S., K.S., M.S.H., D.J.M., Y.T. performed experiments.

722 Y-T.L., K.D.D., F.B-C., N.S., K.S., M.S.H., D.J.M., Y.T. analyzed the data. Y-T.L., K.D.D., M.S.H, D.J.M, and

723 Y.T., wrote the manuscript.

724

725 **Funding**

726 This project was supported by a National Science Foundation (NSF) grant (IOS0950964 and IOS1557936) to

727 Y.T., USDA grant 2012-67013-19361 to M.S.H., UNC-CH start-up funds to D.J. M.

728

729 **Data availability**

730 FAIRE-seq data have been deposited at Gene Expression Omnibus (GEO) under accession number GSE104495.

731

732 REFERENCES

- 733 **Angelini, D. R., Smith, F. W. and Jockusch, E. L.** (2012). Extent With Modification: Leg Patterning in
734 the Beetle *Tribolium castaneum* and the Evolution of Serial Homologs. *G3* **2**, 235–248.
- 735 **Belles, X.** (2010). Beyond *Drosophila*: RNAi in vivo and functional genomics in insects. *Annu Rev*
736 *Entomol* **55**, 111–128.
- 737 **Bischof, J., Maeda, R. K., Hediger, M., Karch, F. and Basler, K.** (2007). An optimized transgenesis
738 system for *Drosophila* using germ-line-specific phiC31 integrases. *Proc. Natl. Acad. Sci. U. S. A.*
739 **104**, 3312–7.
- 740 **Brown, S. J., Mahaffey, J. P., Lorenzen, M. D., Denell, R. E. and Mahaffey, J. W.** (1999). Using
741 RNAi to investigate orthologous homeotic gene function during development of distantly related
742 insects. *Evol Dev* **1**, 11–15.
- 743 **Bucher, G., Scholten, J. and Klingler, M.** (2002). Parental RNAi in *Tribolium* (Coleoptera). *Curr Biol*
744 **12**, R85–6.
- 745 **Cande, J., Goltsev, Y. and Levine, M. S.** (2009). Conservation of enhancer location in divergent
746 insects. *Proc. Natl. Acad. Sci.* **106**, 14414–14419.
- 747 **Carroll, S. B.** (2008). Evo-Devo and an Expanding Evolutionary Synthesis: A Genetic Theory of
748 Morphological Evolution. *Cell* **134**, 25–36.
- 749 **Carroll, S., Grenier, J. K. and Weatherbee, S. D.** (2005). *From DNA to Diversity*. second edi.
750 Blackwell publishing.
- 751 **Chung, Y. T. and Keller, E. B.** (1990). Positive and negative regulatory elements mediating
752 transcription from the *Drosophila melanogaster* actin 5C distal promoter. *Mol. Cell. Biol.* **10**,
753 6172–80.
- 754 **Clark-Hachtel, C. M., Linz, D. M. and Tomoyasu, Y.** (2013). Insights into insect wing origin provided
755 by functional analysis of vestigial in the red flour beetle, *Tribolium castaneum*. *Proc Natl Acad Sci*
756 *U S A* **110**, 16951–16956.
- 757 **Denell, R.** (2008). Establishment of *tribolium* as a genetic model system and its early contributions to
758 evo-devo. *Genetics* **180**, 1779–1786.
- 759 **Eckert, C., Aranda, M., Wolff, C. and Tautz, D.** (2004). Separable stripe enhancer elements for the
760 pair-rule gene hairy in the beetle *Tribolium*. *EMBO Rep.* **5**, 638–42.
- 761 **Frazer, K. A., Pachter, L., Poliakov, A., Rubin, E. M. and Dubchak, I.** (2004). VISTA: computational
762 tools for comparative genomics. *Nucleic Acids Res.* **32**, W273–W279.
- 763 **Giresi, P. G., Kim, J., McDaniel, R. M., Iyer, V. R. and Lieb, J. D.** (2007). FAIRE
764 (Formaldehyde-Assisted Isolation of Regulatory Elements) isolates active regulatory elements
765 from human chromatin. *Genome Res.* **17**, 877–85.
- 766 **Halfon, M. S.** (2017). Perspectives on Gene Regulatory Network Evolution. *Trends Genet.*
- 767 **Hong, J.-W., Hendrix, D. A. and Levine, M. S.** (2008). Shadow enhancers as a source of evolutionary
768 novelty. *Science* **321**, 1314.
- 769 **Horn, C. and Wimmer, E. A.** (2000). A versatile vector set for animal transgenesis. *Dev. Genes Evol.*
770 **210**, 630–7.
- 771 **Jenett, A., Rubin, G. M., Ngo, T.-T. B., Shepherd, D., Murphy, C., Dionne, H., Pfeiffer, B. D.,**
772 **Cavallaro, A., Hall, D., Jeter, J., et al.** (2012). A GAL4-driver line resource for *Drosophila*
773 neurobiology. *Cell Rep.* **2**, 991–1001.
- 774 **Jory, A., Estella, C., Giorgianni, M. W., Slattery, M., Laverly, T. R., Rubin, G. M. and Mann, R. S.**
775 (2012). A survey of 6,300 genomic fragments for cis-regulatory activity in the imaginal discs of
776 *Drosophila melanogaster*. *Cell Rep.* **2**, 1014–24.
- 777 **Juven-Gershon, T., Cheng, S. and Kadonaga, J. T.** (2006). Rational design of a super core promoter
778 that enhances gene expression. *Nat. Methods* **3**, 917–22.
- 779 **Kantorovitz, M. R., Kazemian, M., Kinston, S., Miranda-Saavedra, D., Zhu, Q., Robinson, G. E.,**
780 **Göttgens, B., Halfon, M. S. and Sinha, S.** (2009). Motif-blind, genome-wide discovery of
781 cis-regulatory modules in *Drosophila* and mouse. *Dev. Cell* **17**, 568–79.
- 782 **Katzen, F.** (2007). Gateway[®] recombinational cloning: a biological operating system. *Expert Opin.*

- 783 *Drug Discov.* **2**, 571–589.
- 784 **Kazemian, M., Zhu, Q., Halfon, M. S. and Sinha, S.** (2011). Improved accuracy of supervised CRM
785 discovery with interpolated Markov models and cross-species comparison. *Nucleic Acids Res.* **39**,
786 9463–72.
- 787 **Kazemian, M., Suryamohan, K., Chen, J.-Y., Zhang, Y., Samee, M. A. H., Halfon, M. S. and Sinha,**
788 **S.** (2014). Evidence for deep regulatory similarities in early developmental programs across
789 highly diverged insects. *Genome Biol. Evol.* **6**, 2301–20.
- 790 **Kvon, E. Z., Kazmar, T., Stampfel, G., Yáñez-Cuna, J. O., Pagani, M., Schernhuber, K., Dickson, B.**
791 **J. and Stark, A.** (2014). Genome-scale functional characterization of *Drosophila* developmental
792 enhancers in vivo. *Nature* **512**, 91–5.
- 793 **Li, L., Zhu, Q., He, X., Sinha, S. and Halfon, M. S.** (2007). Large-scale analysis of transcriptional
794 cis-regulatory modules reveals both common features and distinct subclasses. *Genome Biol* **8**,
795 R101.
- 796 **Lorenzen, M. D., Berghammer, A. J., Brown, S. J., Denell, R. E., Klingler, M. and Beeman, R. W.**
797 (2003). piggyBac-mediated germline transformation in the beetle *Tribolium castaneum*. *Insect*
798 *Mol Biol* **12**, 433–440.
- 799 **Lynch, J. A., El-Sherif, E. and Brown, S. J.** (2012). Comparisons of the embryonic development of
800 *Drosophila*, *Nasonia*, and *Tribolium*. *Wiley Interdiscip. Rev. Dev. Biol.* **1**, 16–39.
- 801 **Marques-Souza, H.** (2007). Evolution of the gene regulatory network controlling trunk segmentation in
802 insects.
- 803 **Marques-Souza, H., Aranda, M. and Tautz, D.** (2008). Delimiting the conserved features of
804 hunchback function for the trunk organization of insects. *Development* **135**, 881–888.
- 805 **Mayor, C., Brudno, M., Schwartz, J. R., Poliakov, A., Rubin, E. M., Frazer, K. A., Pachter, L. S. and**
806 **Dubchak, I.** (2000). VISTA : visualizing global DNA sequence alignments of arbitrary length.
807 *Bioinformatics* **16**, 1046–7.
- 808 **McKay, D. J. and Lieb, J. D.** (2013). A common set of DNA regulatory elements shapes *Drosophila*
809 appendages. *Dev. Cell* **27**, 306–18.
- 810 **Monteiro, A. and Podlaha, O.** (2009). Wings, Horns, and Butterfly Eyespots: How Do Complex Traits
811 Evolve? *PLoS Biol.* **7**, e1000037.
- 812 **Ng, M., Diaz-Benjumea, F. J. and Cohen, S. M.** (1995). Nubbin encodes a POU-domain protein
813 required for proximal-distal patterning in the *Drosophila* wing. *Development* **121**, 589–599.
- 814 **Pearson, J. C., McKay, D. J., Lieb, J. D. and Crews, S. T.** (2016). Chromatin profiling of *Drosophila*
815 CNS subpopulations identifies active transcriptional enhancers. *Development* **143**, 3723–3732.
- 816 **Peel, A. D.** (2008). The evolution of developmental gene networks: lessons from comparative studies
817 on holometabolous insects. *Philos. Trans. R. Soc. B Biol. Sci.* **363**, 1539–1547.
- 818 **Pfeiffer, B. D., Jenett, A., Hammonds, A. S., Ngo, T.-T. B., Misra, S., Murphy, C., Scully, A.,**
819 **Carlson, J. W., Wan, K. H., Laverly, T. R., et al.** (2008). Tools for neuroanatomy and
820 neurogenetics in *Drosophila*. *Proc. Natl. Acad. Sci. U. S. A.* **105**, 9715–20.
- 821 **Quinlan, A. R. and Hall, I. M.** (2010). BEDTools: a flexible suite of utilities for comparing genomic
822 features. *Bioinformatics* **26**, 841–2.
- 823 **Robinson, J. T., Thorvaldsdóttir, H., Winckler, W., Guttman, M., Lander, E. S., Getz, G. and**
824 **Mesirov, J. P.** (2011). Integrative genomics viewer. *Nat. Biotechnol.* **29**, 24–26.
- 825 **Schinko, J. B., Weber, M., Viktorinova, I., Kiupakis, A., Averof, M., Klingler, M., Wimmer, E. A.**
826 **and Bucher, G.** (2010). Functionality of the GAL4/UAS system in *Tribolium* requires the use of
827 endogenous core promoters. *BMC Dev Biol* **10**, 53.
- 828 **Schmitt-Engel, C., Schultheis, D., Schwirz, J., Ströhlein, N., Troelenberg, N., Majumdar, U., Dao,**
829 **V. A., Grossmann, D., Richter, T., Tech, M., et al.** (2015). The iBeetle large-scale RNAi screen
830 reveals gene functions for insect development and physiology. *Nat. Commun.* **6**, 7822.
- 831 **Shippy, T. D., Coleman, C. M., Tomoyasu, Y. and Brown, S. J.** (2009). Concurrent in situ
832 hybridization and antibody staining in red flour beetle (*Tribolium*) embryos. *Cold Spring Harb*
833 *Protoc* **2009**, pdb prot5257.
- 834 **Shlyueva, D., Stampfel, G. and Stark, A.** (2014). Transcriptional enhancers: from properties to
835 genome-wide predictions. *Nat. Rev. Genet.* **15**, 272–286.

- 836 **Simon, J. M., Giresi, P. G., Davis, I. J. and Lieb, J. D.** (2012). Using formaldehyde-assisted isolation
837 of regulatory elements (FAIRE) to isolate active regulatory DNA. *Nat. Protoc.* **7**, 256–267.
- 838 **Smith, F. W., Angelini, D. R., Gaudio, M. S. and Jockusch, E. L.** (2014). Metamorphic labral axis
839 patterning in the beetle *Tribolium castaneum* requires multiple upstream, but few downstream,
840 genes in the appendage patterning network. *Evol. Dev.* **16**, 78–91.
- 841 **Song, L., Zhang, Z., Grasfeder, L. L., Boyle, A. P., Giresi, P. G., Lee, B.-K., Sheffield, N. C., Gräf,
842 S., Huss, M., Keefe, D., et al.** (2011). Open chromatin defined by DNaseI and FAIRE identifies
843 regulatory elements that shape cell-type identity. *Genome Res.* **21**, 1757–67.
- 844 **Sosinsky, A., Honig, B., Mann, R. S. and Califano, A.** (2007). Discovering transcriptional regulatory
845 regions in *Drosophila* by a nonalignment method for phylogenetic footprinting. *Proc Natl Acad Sci*
846 *U S A* **104**, 6305–6310.
- 847 **Stark, A., Lin, M. F., Kheradpour, P., Pedersen, J. S., Parts, L., Carlson, J. W., Crosby, M. A.,
848 Rasmussen, M. D., Roy, S., Deoras, A. N., et al.** (2007). Discovery of functional elements in 12
849 *Drosophila* genomes using evolutionary signatures. *Nature* **450**, 219–232.
- 850 **Suryamohan, K. and Halfon, M. S.** (2015). Identifying transcriptional *cis*-regulatory modules in
851 animal genomes. *Wiley Interdiscip. Rev. Dev. Biol.* **4**, 59–84.
- 852 **Thorvaldsdóttir, H., Robinson, J. T. and Mesirov, J. P.** (2013). Integrative Genomics Viewer (IGV):
853 high-performance genomics data visualization and exploration. *Brief. Bioinform.* **14**, 178–92.
- 854 **Tomoyasu, Y.** (2017). Ultrabithorax and the evolution of insect forewing/hindwing differentiation. *Curr.*
855 *Opin. Insect Sci.* **19**,.
- 856 **Tomoyasu, Y. and Denell, R. E.** (2004). Larval RNAi in *Tribolium* (Coleoptera) for analyzing adult
857 development. *Dev Genes Evol* **214**, 575–578.
- 858 **Tomoyasu, Y., Wheeler, S. R. and Denell, R. E.** (2005). Ultrabithorax is required for membranous
859 wing identity in the beetle *Tribolium castaneum*. *Nature* **433**, 643–647.
- 860 **Tomoyasu, Y., Arakane, Y., Kramer, K. J. and Denell, R. E.** (2009). Repeated Co-options of
861 Exoskeleton Formation during Wing-to-Elytron Evolution in Beetles. *Curr. Biol.* **19**, 2057–2065.
- 862 **Tribolium Genome Sequencing consortium, C., Richards, S., Gibbs, R. A., Weinstock, G. M.,
863 Brown, S. J., Denell, R., Beeman, R. W., Gibbs, R., Beeman, R. W., Brown, S. J., et al.** (2008).
864 The genome of the model beetle and pest *Tribolium castaneum*. *Nature* **452**, 949–955.
- 865 **Uyehara, C. M., Nystrom, S. L., Niederhuber, M. J., Leatham-Jensen, M., Ma, Y., Buttitta, L. A.
866 and McKay, D. J.** (2017). Hormone-dependent control of developmental timing through
867 regulation of chromatin accessibility. *Genes Dev.* **31**, 862–875.
- 868 **Wang, L., Wang, S., Li, Y., Paradesi, M. S. and Brown, S. J.** (2007). BeetleBase: the model organism
869 database for *Tribolium castaneum*. *Nucleic Acids Res* **35**, D476-9.
- 870 **Wolff, C., Schröder, R., Schulz, C., Tautz, D. and Klingler, M.** (1998). Regulation of the *Tribolium*
871 homologues of caudal and hunchback in *Drosophila*: evidence for maternal gradient systems in a
872 short germ embryo. *Development* **125**, 3645–54.
- 873 **Zabidi, M. A., Arnold, C. D., Schernhuber, K., Pagani, M., Rath, M., Frank, O. and Stark, A.** (2015).
874 Enhancer-core-promoter specificity separates developmental and housekeeping gene regulation.
875 *Nature* **518**, 556–9.
- 876 **Zdobnov, E. M. and Bork, P.** (2007). Quantification of insect genome divergence. *Trends Genet.* **23**,
877 16–20.
- 878 **Zhu, X., Rudolf, H., Healey, L., François, P., Brown, S. J., Klingler, M. and El-Sherif, E.** (2017).
879 Speed regulation of genetic cascades allows for evolvability in the body plan specification of
880 insects. *Proc. Natl. Acad. Sci. U. S. A.* 201702478.
- 881 **Zinzen, R. P., Cande, J., Ronshaugen, M., Papatsenko, D. and Levine, M.** (2006). Evolution of the
882 Ventral Midline in Insect Embryos. *Dev. Cell* **11**, 895–902.

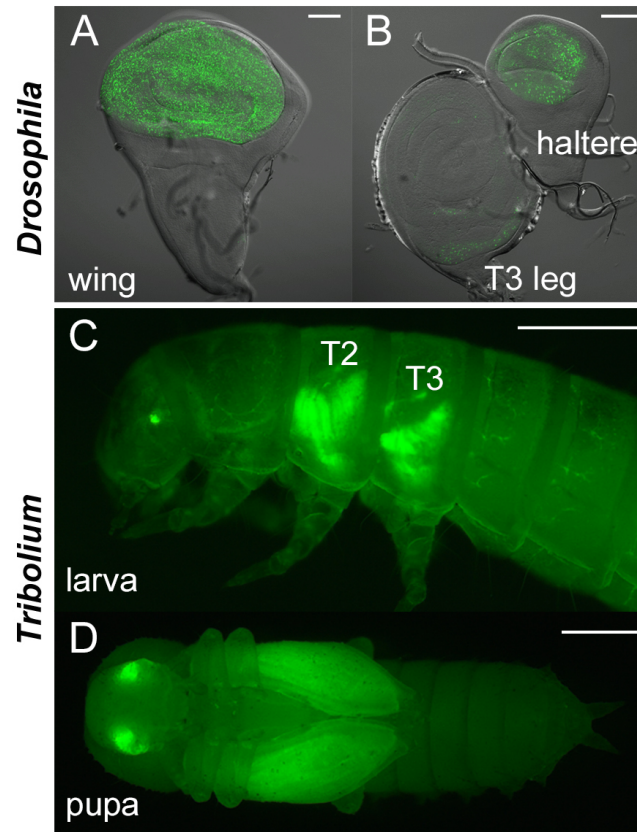
883

884

885 **FIGURES**

886

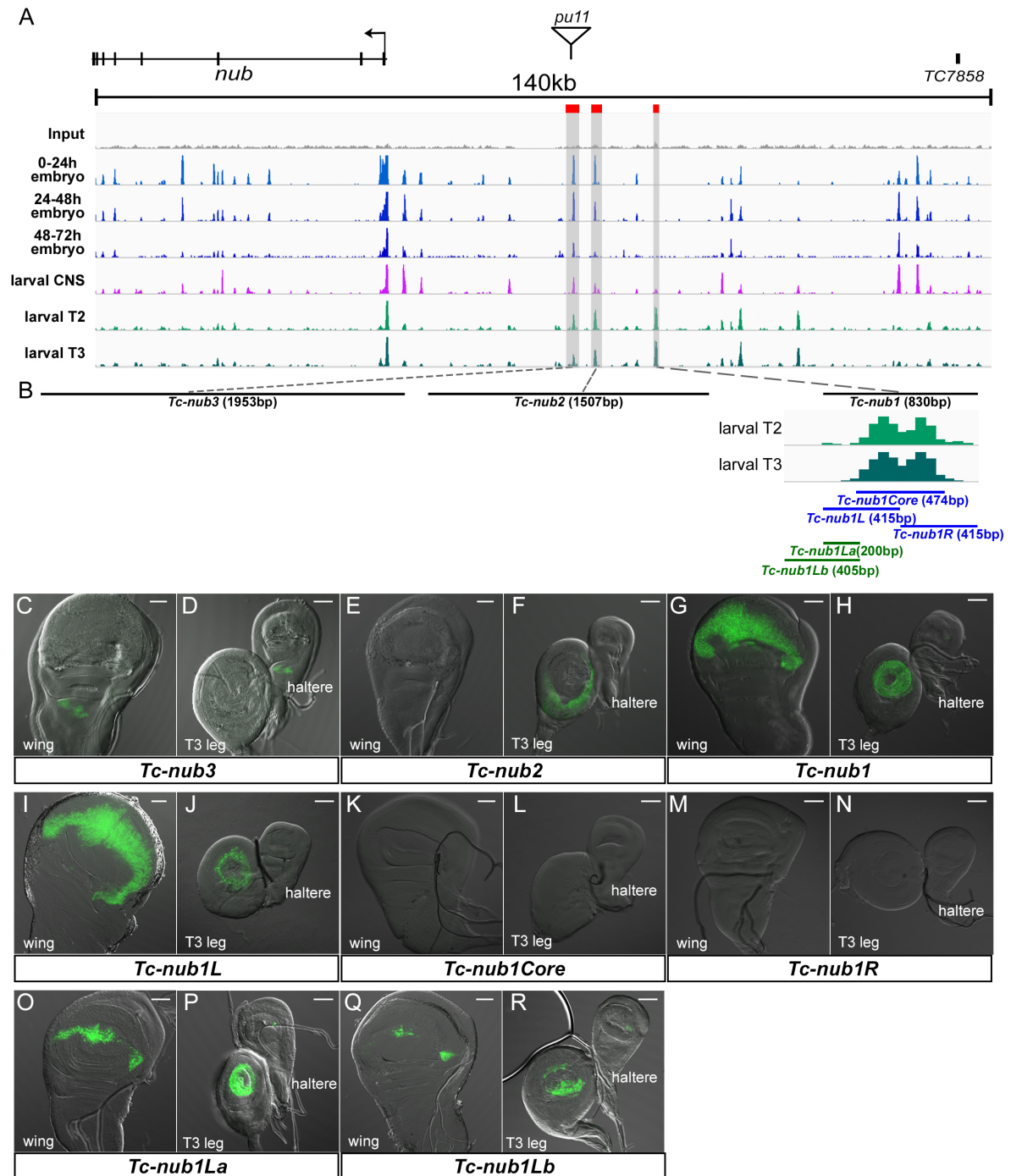
887



888

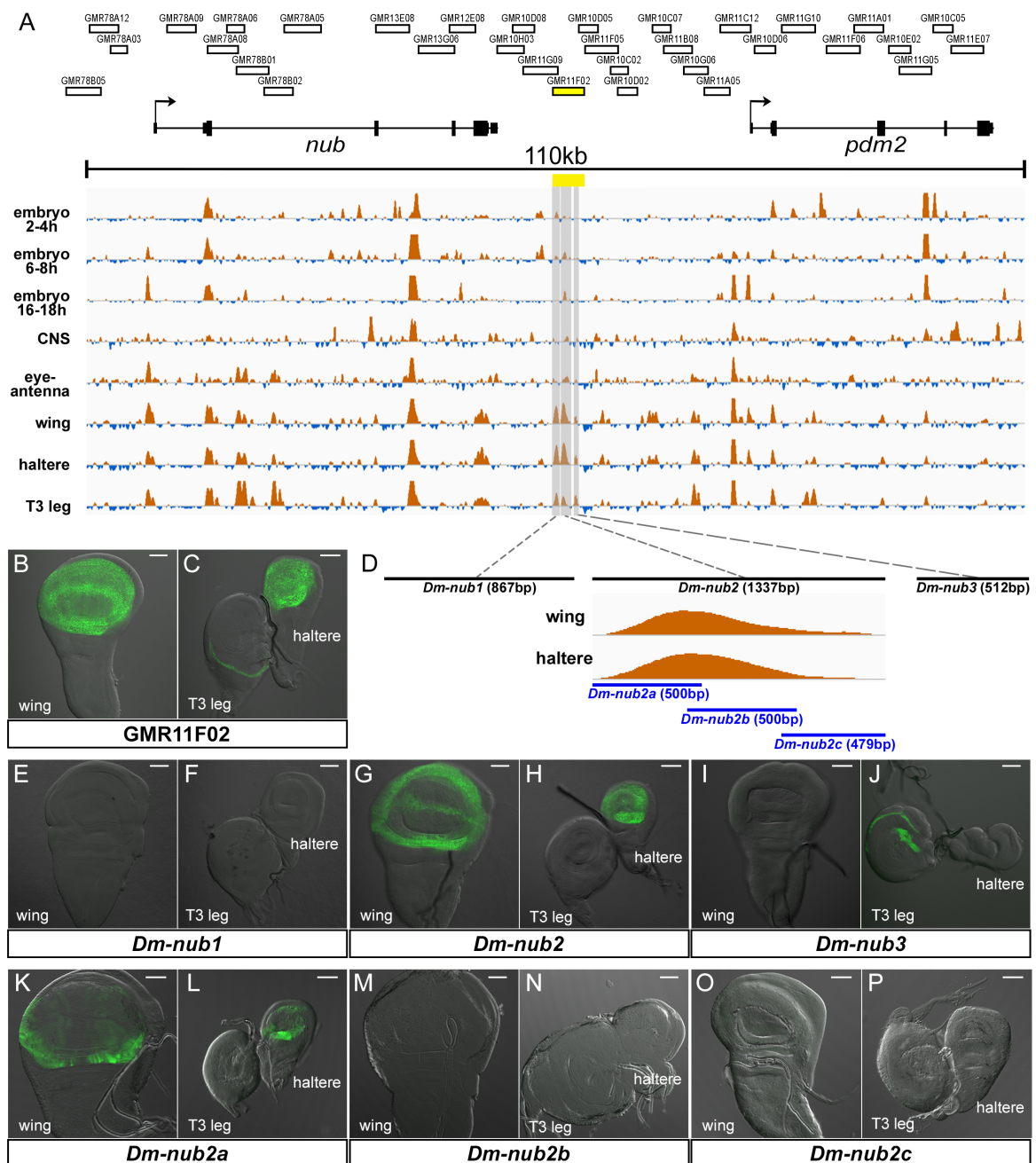
889 **Fig. 1. *nub* enhancer trap expression in *Drosophila* and *Tribolium*.** (A, B) The
890 *nub* enhancer trap expression in the wing disc (A), and the haltere and T3 leg discs (B)
891 in *Drosophila*. (C, D) Expression pattern of the *nub* enhancer trap line (*pu11*) at the
892 larval (C) and pupal (D) stage in *Tribolium*. Scale bar: 0.5mm.

893



894
895
896
897
898
899
900
901
902
903

Fig. 2. Identification of the *Tribolium nub* wing enhancer with FAIRE and inter-species reporter assay. (A) FAIRE profiles at the *Tribolium nub* locus in six different tissues/stages. The *pu11* insertion site is indicated with a triangle. Three peaks near the *pu11* insertion site chosen for evaluating enhancer activity were marked with red boxes. (B) Summary of the regions tested by the reporter assay. The distance between *Tc-nub1*, *2*, and *3* are not scaled. The magnified view of the FAIRE peak corresponding to *Tc-nubL1* is also presented. (C-R) Enhancer activity of each *Tribolium* genomic region tested in the *Drosophila* imaginal discs. Scale bar: 50 μ m.



904

905

Fig. 3. Identification of the *Drosophila nub* wing enhancer. (A)

906

FAIRE profiles from eight different tissues/stages at the *nub* and *pdm2* loci in *Drosophila*. The regions surveyed in the FlyLight project are also indicated. The region that shows wing enhancer activity is marked by yellow.

907

(B, C) Expression driven by GMR11F02 in the *Drosophila* imaginal discs. (D)

908

Summary of the regions within GMR11F02 tested by the reporter assay. The relative distance between *Dm-nub1*, 2, and 3 are not scaled. The magnified view of the

909

Dm-nub2 peak is also included. (E-P) Enhancer activity of each *Drosophila* genomic region tested in the *Drosophila* imaginal discs. Scale bar: 50 μ m.

910

(E-P) Enhancer activity of each *Drosophila* genomic region tested in the *Drosophila* imaginal discs. Scale bar: 50 μ m.

911

(E-P) Enhancer activity of each *Drosophila* genomic region tested in the *Drosophila* imaginal discs. Scale bar: 50 μ m.

912

(E-P) Enhancer activity of each *Drosophila* genomic region tested in the *Drosophila* imaginal discs. Scale bar: 50 μ m.

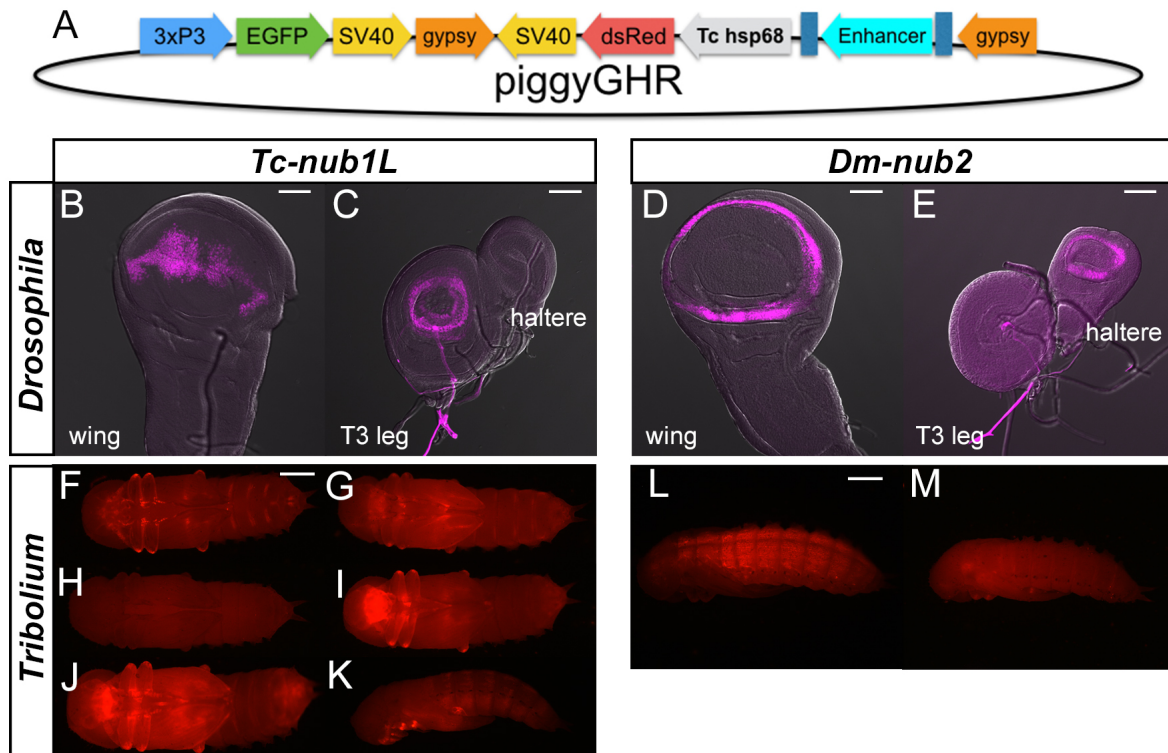
913

(E-P) Enhancer activity of each *Drosophila* genomic region tested in the *Drosophila* imaginal discs. Scale bar: 50 μ m.

914

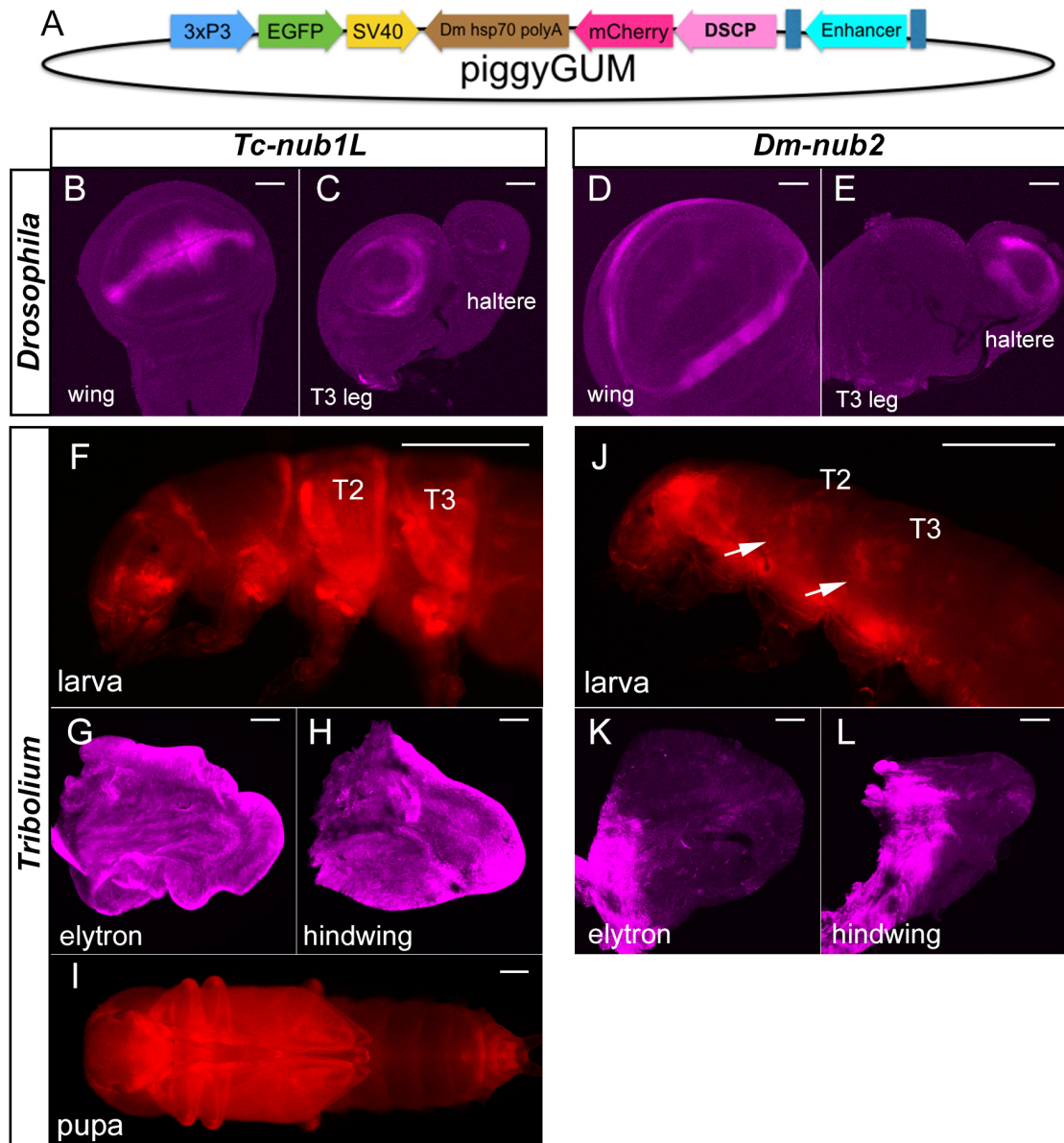
(E-P) Enhancer activity of each *Drosophila* genomic region tested in the *Drosophila* imaginal discs. Scale bar: 50 μ m.

915
916
917
918
919



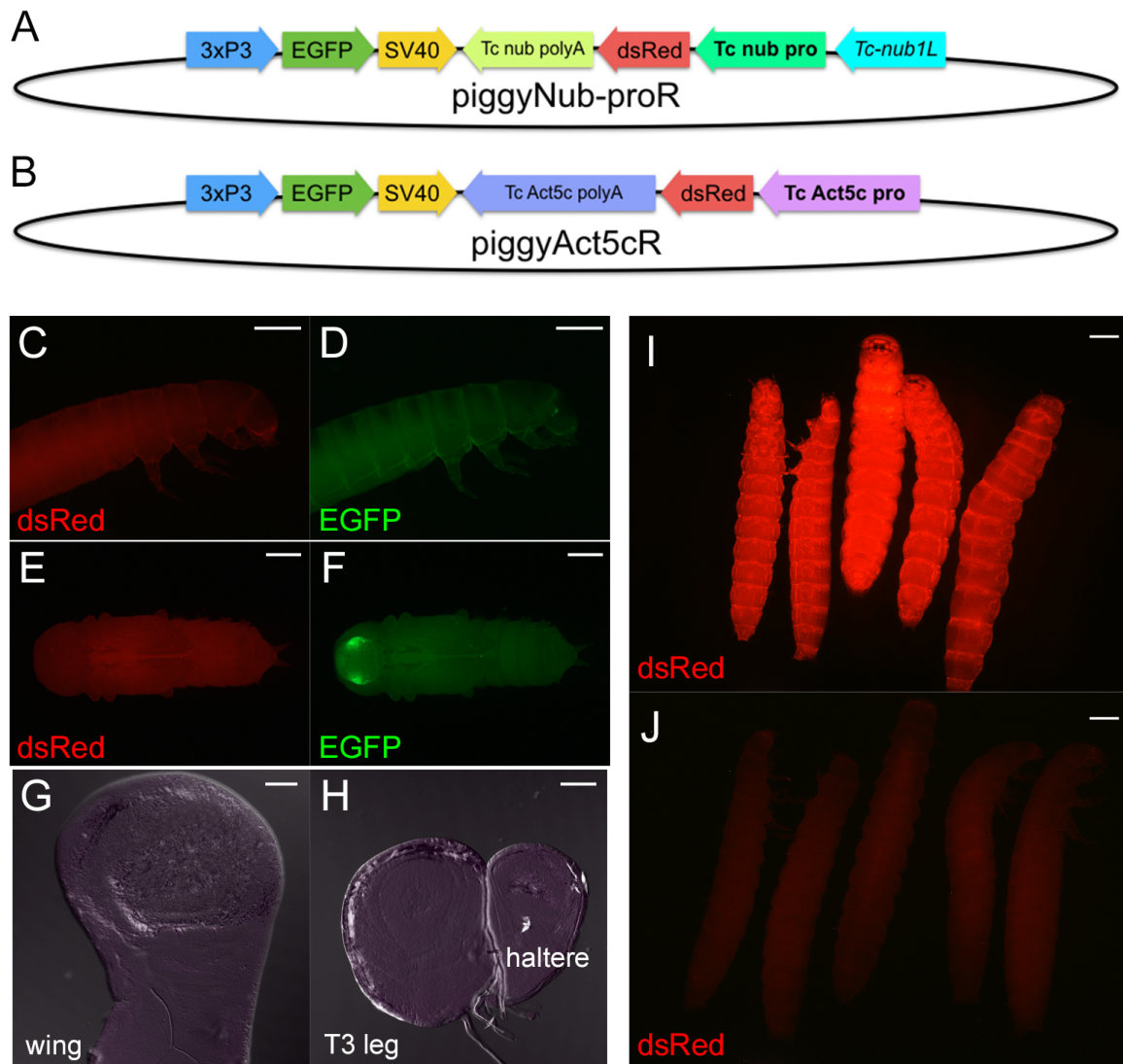
920
921
922
923
924
925
926
927

Fig. 4. Reporter assay with the *Tc-hsp68* promoter construct in *Drosophila* and *Tribolium*. (A) The piggyGHR construct. (B-E) Enhancer activity of *Tc-Nub1L* (B, C) and *Dm-nub2* (D, E) tested with the piggyGHR construct in *Drosophila*. (F-M) Enhancer activity of *Tc-nub1L* (F-K) and *Dm-nub2* (L, M) tested with piggyGHR at the pupal stage in *Tribolium*. Six independent lines for *Tc-nub1L* (F-K) and two for *Dm-nub2* (L, M) were shown. Scale bar: 50 μ m (B-E), 0.5 mm (F-M)



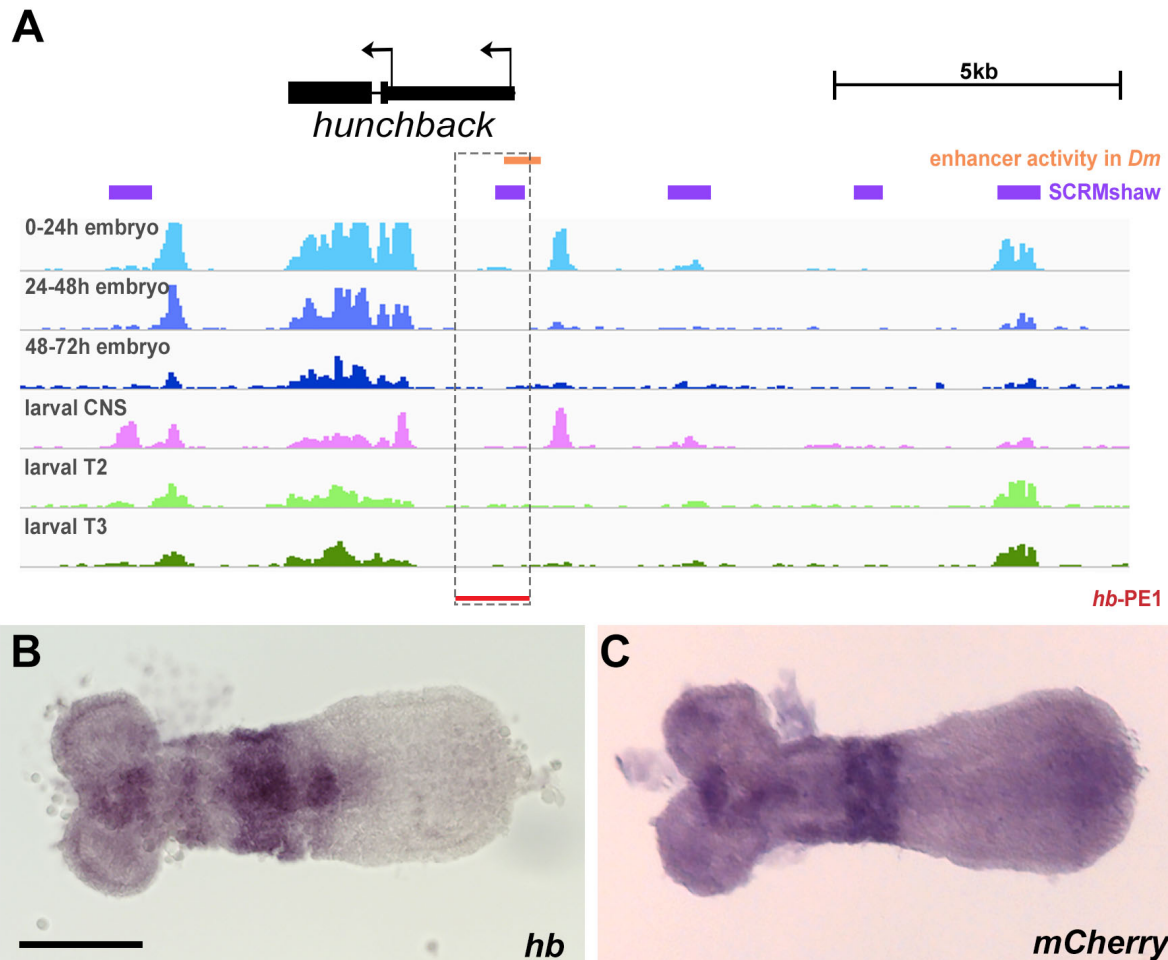
928
929
930
931
932
933
934
935

Fig. 5. Reporter assay with the *Drosophila* synthetic core promoter construct in *Drosophila* and *Tribolium*. (A) The piggyGUM construct. (B-E) Enhancer activity of *Tc-Nub1L* (B, C) and *Dm-nub2* (D, E) tested with the piggyGUM construct in *Drosophila*. (F-L) Reporter expression of piggyGUM-*Tc-nub1L* (F-I) and piggyGUM-*Dm-nub2* (J-L) in *Tribolium*. Scale bar: 50 μ m (B-E, G, H, K, L), 0.5 mm (F, J, I)



936
937
938
939
940
941
942
943
944
945
946
947

Fig. 6. Reporter assay with the *Tribolium* endogenous promoters in *Drosophila* and *Tribolium*. (A) The piggyNub-proR construct. (B) The piggyAct5cR construct. (C-F) Enhancer activity of *Tc-Nub1L* tested with the piggyNub-proR construct. dsRed reporter expression is completely absent (C, E), even though EGFP (D, F) confirms the presence of the construct transgened. (G, H) The piggyNub-proR reporter expression in *Drosophila* imaginal discs. (I) dsRed expression of the piggyAct5cR at the larval stage in *Tribolium*. (J) dsRed expression of the piggyNub-proR with *Tc-Nub1L* at the larval stage in *Tribolium*, with the same exposure time as (I). Scale bar: 0.5 mm (C-F, I, J), 50 μ m (G, H).



948
949
950
951
952
953
954
955

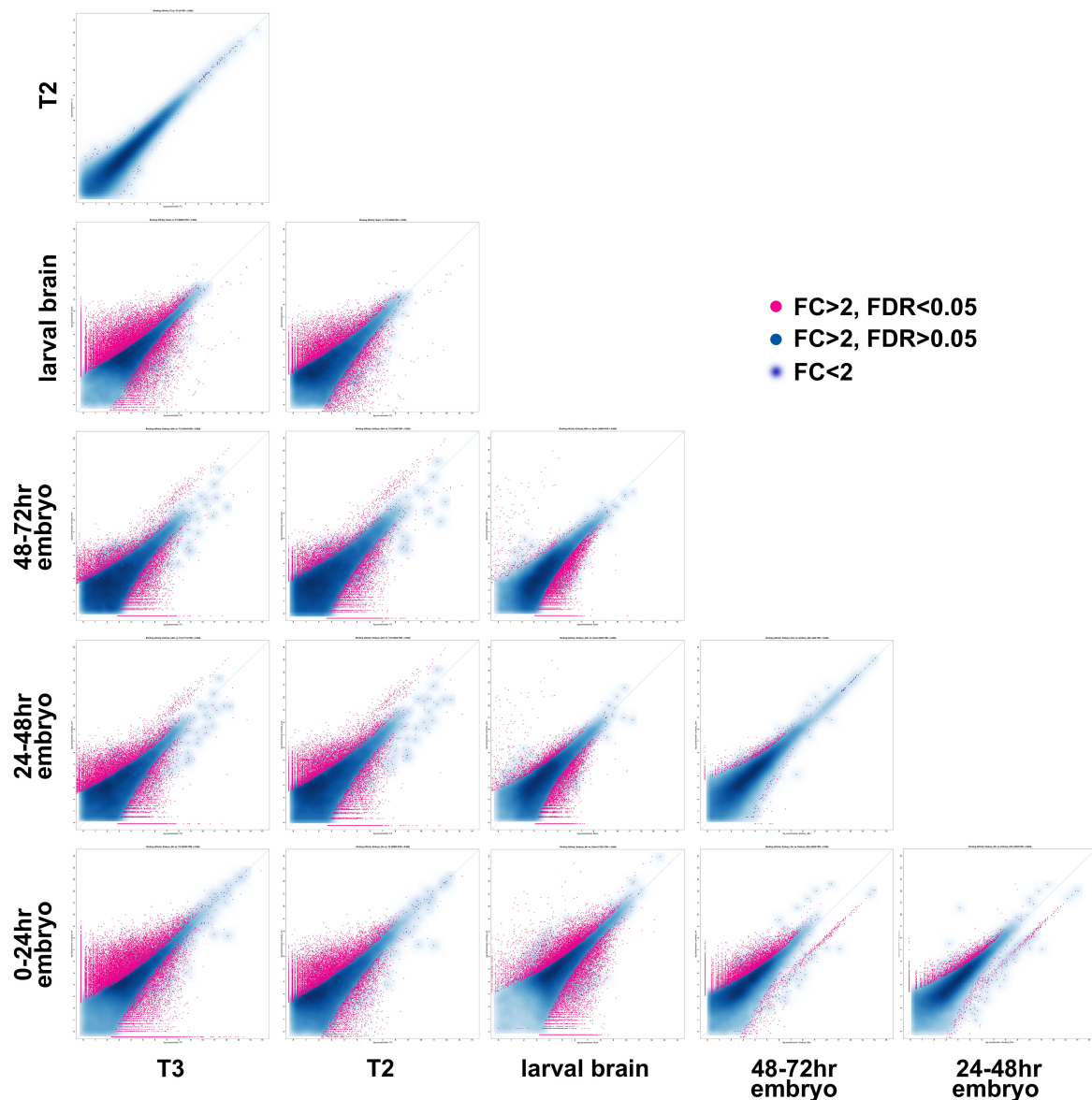
Fig. 7. *hb* enhancer analysis in *Tribolium*. (A) FAIRE profiles at the *hb* locus. Orange bar: blastoderm enhancer activity when introduced in *Drosophila*, purple bars: SCRMshaw predictions, red bar: the 1340bp fragment tested in this study (*hb-PE1*). (B) *hb* expression at the early germband stage detected by *in situ* hybridization for *hb* transcript. (C) *mCherry* reporter gene expression of piggyGUM-*hb-PE1* detected by *in situ* hybridization for *mCherry* transcript. Scale bar: 100 μ m (B, C).

T2	1 / 3				
brain	15427 / 7262	11634 / 5258			
48-72hr	6428 / 8134	5575 / 7259	1602 / 4089		
24-48hr	10380 / 6729	9572 / 6031	3162 / 6689	863 / 40	
0-24hr	17450 / 8800	14138 / 6808	9002 / 8279	7651 / 1041	2407 / 586
	T3	T2	brain	48-72hr	24-48hr

956
957
958
959

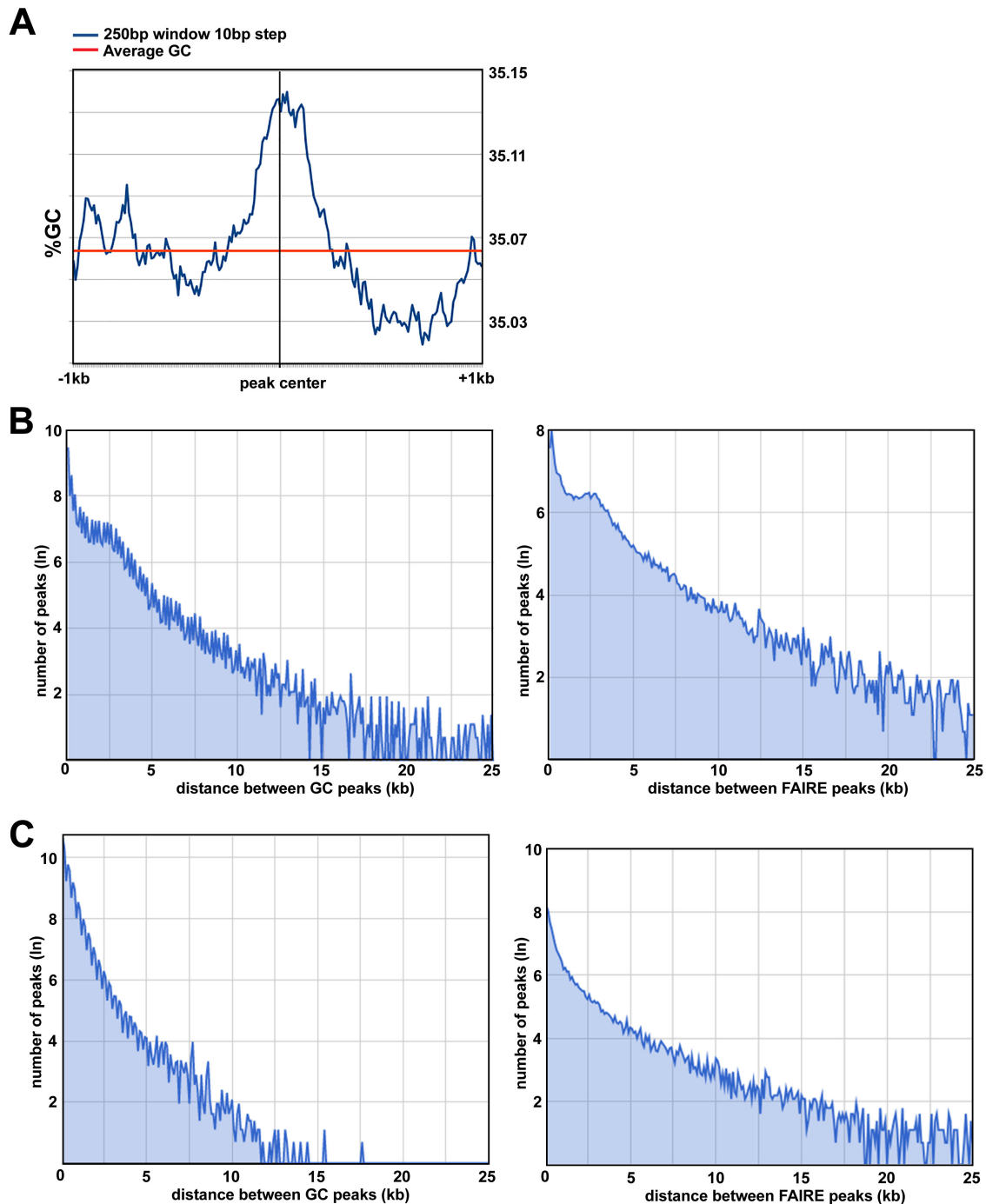
Table 1. The number of differentially open peaks

960 **SUPPLEMENTAL FIGURES**



961
962
963
964
965
966
967

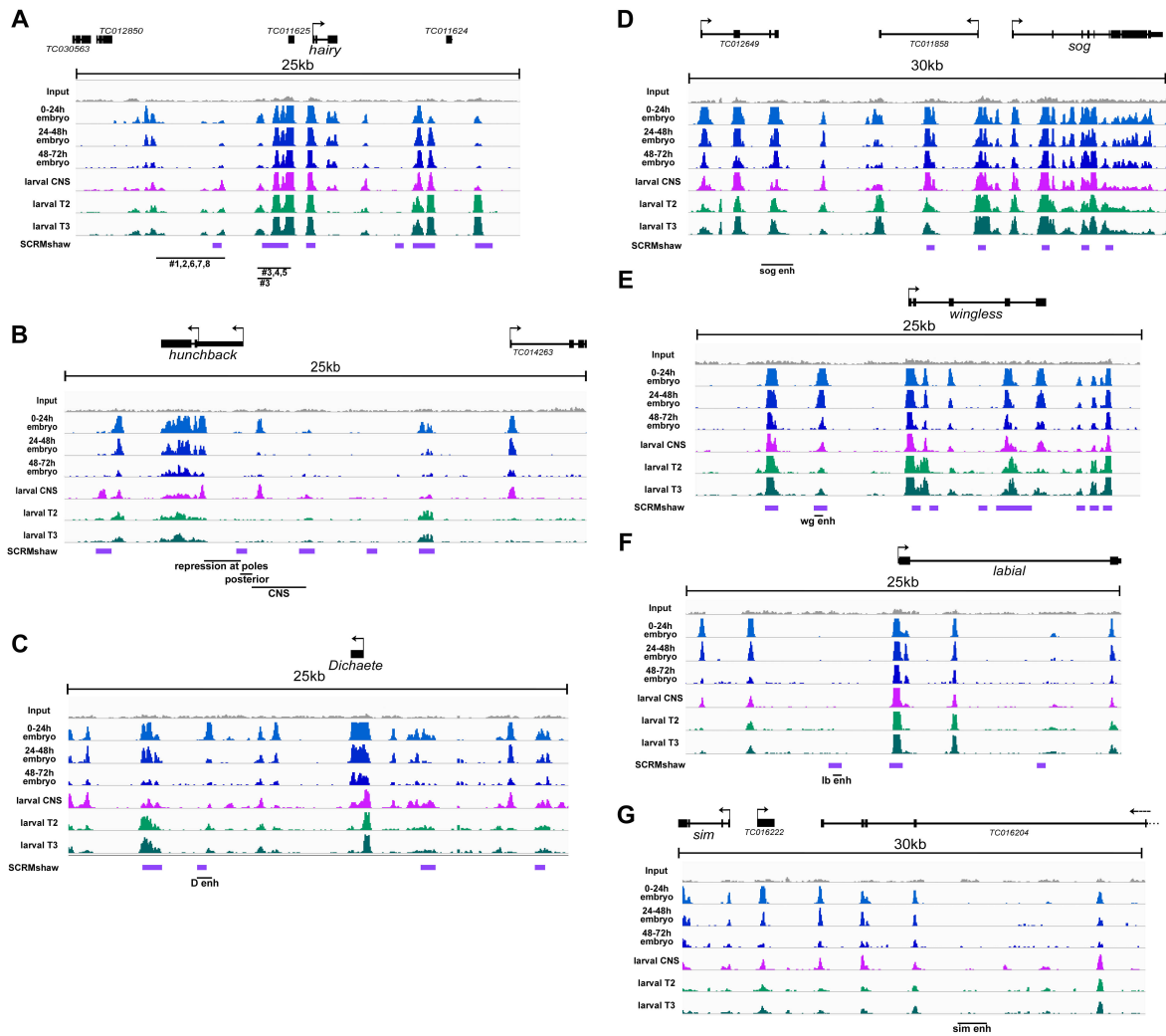
Fig. S1. Differentially open peak analysis. Pairwise analysis of differentially open peaks between samples. Red represents peaks that exhibit over two-fold change (FC) between samples with the false discovery rate (FDR) < 0.05, while blue represents peaks over two-fold change but with FDR > 0.05. The blue cloud represents peaks with less than two-fold change between samples.



968
969
970
971
972
973
974
975

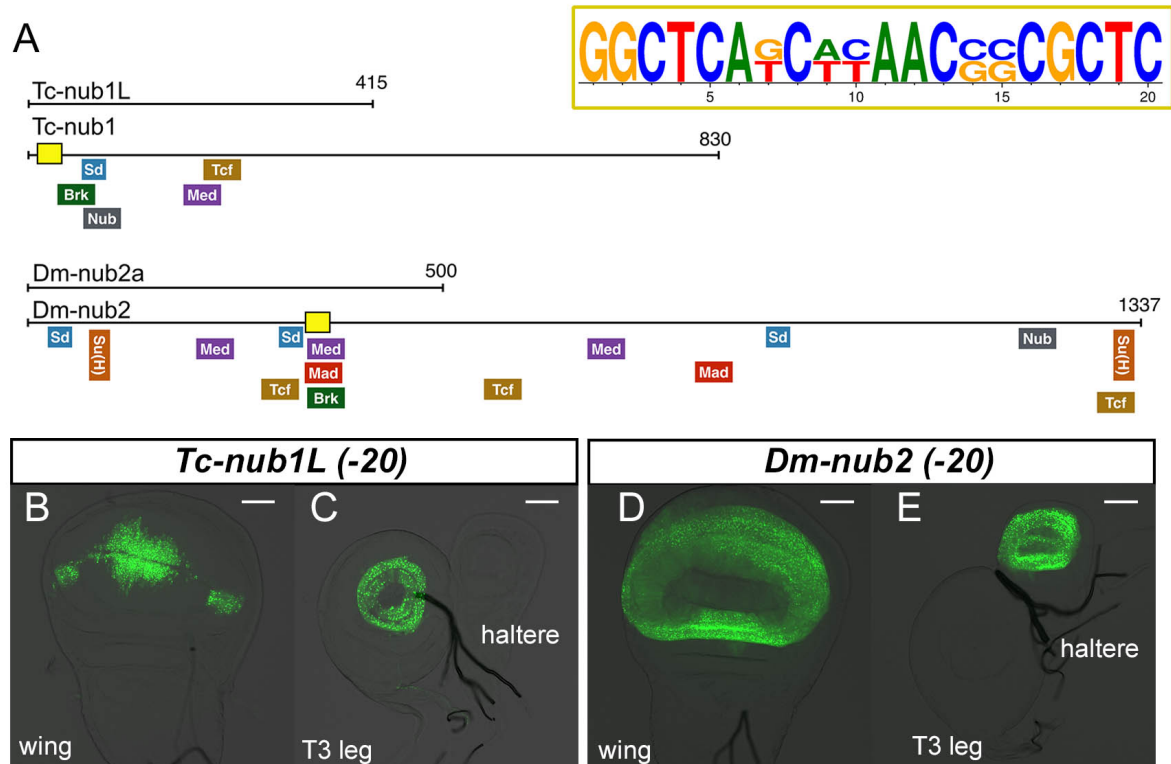
Fig. S2. Distribution of FAIRE peaks and GC-rich regions.

(A) Correlation between FAIRE peaks and high GC contents in *Tribolium*. (B) Distribution of intervals between FAIRE peaks in *Tribolium* and *Drosophila*. (C) Distribution of intervals between GC-rich regions in *Tribolium* and *Drosophila*. Note that there is a significant accumulation around 3 kb in *Tribolium* but not in *Drosophila* (B, C).



976
977
978
979
980
981
982
983
984
985
986
987

Fig. S3. Comparison of the FAIRE data to previous enhancer studies. (A) *hairy* (*h*), (B) *hunchback* (*hb*), (C) *Dichaete* (*D*), (D) *short gastrulation* (*sog*), (E) *wingless* (*wg*), (F) *labial* (*lab*), (G) *single-minded* (*sim*). Previously described possible enhancer regions at these loci are shown by black lines underneath the FAIRE profiles. SCRMshaw predictions are also shown (purple). Only the enhancers at the *h* locus have been tested in the native *Tribolium* context, while other enhancers were evaluated in the cross-species context. FAIRE peaks match well with the previously described enhancers for *h*, *hb*, *D*, *sog*, and *wg* (A-E), while no significant overlaps are observed between FAIRE peaks and the previously described enhancers for *lab* and *sim*.



988
989
990
991
992
993
994
995
996
997

Fig. S4. Deletion of the motif shared between the *Tribolium* and *Drosophila nub* wing enhancers. (A) Locations of TF binding sites within the *Tribolium* and *Drosophila nub* wing enhancers. A 20bp shared sequence between the two enhancers is shown with a yellow box. (B, C) Activities of the *Tribolium* and *Drosophila nub* wing enhancers when the conserved 20bp shared sequence is deleted. No significant changes in enhancer activity are observed, indicating that the 20bp sequence is dispensable from the activity of the two enhancers. Scale bar: 50 μ m.

998 **SUPPLEMENTAL TABLES**

999

Training_set ^a	n ^b	FAIRE 0-24hr	FAIRE 24-48hr	FAIRE 48-72hr	FAIRE larvalT2	FAIRE larvalT3	combined (embryo)	combined (larval)	combined
ap	129	60.5%	55.8%	55.0%	73.6%	72.1%	nd ^c	nd	nd
blastoderm	138	76.1%	72.5%	68.8%	87.0%	89.9%	nd	nd	nd
cns	256	86.7%	82.0%	83.6%	93.4%	93.0%	nd	nd	nd
dorsal_ectoderm	183	79.2%	74.9%	74.3%	88.0%	87.4%	nd	nd	nd
dv	137	69.3%	65.0%	67.2%	86.9%	84.7%	nd	nd	nd
ectoderm+ectoderm.2	280	76.4%	73.6%	74.6%	86.8%	88.2%	nd	nd	nd
endoderm	109	68.8%	63.3%	66.1%	78.0%	82.6%	nd	nd	nd
imaginal_disc (1+2)	246	85.4%	83.3%	81.3%	93.9%	94.3%	nd	nd	nd
mesectoderm	42	83.3%	81.0%	81.0%	97.6%	92.9%	nd	nd	nd
somatic_muscle	42	78.6%	76.2%	81.0%	83.3%	88.1%	nd	nd	nd
ventral_ectoderm	129	89.1%	86.8%	86.8%	90.7%	92.2%	nd	nd	nd
wing.2	99	91.9%	90.9%	90.9%	98.0%	98.0%	nd	nd	nd
all_combined	1214	74.1%	70.5%	71.1%	85.1%	85.3%	78.8%	88.1%	90.3%

^a Training sets as listed in Kazemian et al. (2014). "all_combined" is all 1214 enhancer predictions. Not all individual training sets are shown.

^b Total predicted enhancers

^c nd: not done

1000
1001
1002
1003
1004
1005
1006

Table S1. Overlap between SCRMshaw predictions and FAIRE peaks

Table S2. The list of FARIE peaks that overlap SCRMshaw. (attached separately)

Enhancer	wing	haltere	leg	antennae /eyes	CNS*	trachea	gut	mouthpart	salivary gland*	others
<i>Tc-nub1</i>	DV boundary	a few cells	+	antennae & optical nerves	++	+	++	+	-	a circle of cells near the posterior end
<i>Tc-nub2</i>	-	-	+	antennae	+	-	+	+	+	
<i>Tc-nub3</i>	notum	notum	-	-	+	-	++	+	+	spiracles
<i>Tc-nub1Core</i>	-	-	-	-	+	-	+	+	+	a line of cells in epidermis
<i>Tc-nub1L</i>	DV boundary	a few cells	+	antennae & optical nerves	++	+	+	+	-	
<i>Tc-nub1R</i>	-	-	-	-	+	-	++	-	+	spiracles, a circle of cells near the posterior end
<i>Tc-nub1a</i>	DV boundary	a few cells	+	antennae & optical nerves	++	-	++	+	+	
<i>Tc-nub1Lb</i>	DV boundary	a few cells	+	antennae & optical nerves	++	+	++	+	+	

*CNS and salivary gland expression may not be specific to the construct tested.

1007
1008
1009
1010

Table S3. Expression of *Tc nub* reporter constructs outside of the wing and leg imaginal disc in *Drosophila*

Enhancer	wing	haltere	leg	antennae /eyes	CNS	trachea	gut	mouthpart	Salivary gland
<i>Dm-nub1</i>	-	-	-	-	++	-	++	-	+
<i>Dm-nub2</i>	pouch	pouch	-	-	++	-	++	+	+
<i>Dm-nub3</i>	-	-	++	-	++	-	++	+	+
<i>Dm-nub2a</i>	pouch	pouch	-	+	+	-	+	+	-
<i>Dm-nub2b</i>	-	-	-	-	+	-	+	-	-
<i>Dm-nub2c</i>	-	-	-	-	+	-	++	-	-

*CNS and salivary gland expression may not be specific to the construct tested.

Table S4. Expression of *Dm nub* reporter constructs outside of the wing and leg imaginal disc in *Drosophila*

Fragment	length	primer 1	primer 2
<i>Tc-nub1</i>	830bp	CACCATAATGGGAGGTGGTTAATGG	TATAAGTCGCAGGCTCATCAT
<i>Tc-nub2</i>	1507bp	CACCCATTGTTAAGTGTGTTAAAAA	CAACAATCTATAAAGCTAACG
<i>Tc-nub3</i>	1953bp	CACCAAGACATGATGCTTAATGCTT	ACCTTAATTAATGTATTAACA
<i>Tc-nub1Core</i>	474bp	CACCTTATGTGTCGTCGGGCTTTAT	TTCCGATTGCCGTCTGCGTAT
<i>Tc-nub1L</i>	415bp	CACCCCTGCTGCGACCTTGTGGT	TATAAGTCGCAGGCTCATCAT
<i>Tc-nub1R</i>	415bp	CACCATAATGGGAGGTGGTTAATGG	ACTTATCTTAAGATATGTGC
<i>Tc-nub1La</i>	200bp	TATAAGTCGCAGGCTCATCAT	ACATACGCAGACGGCAATCGGAA
<i>Tc-nub1Lb</i>	405bp	CACCATTTTTTCAGCTGTAATTTAAA	ACATACGCAGACGGCAATCGGAA
<i>Tc-hb PE1</i>	1340bp	CTATTTACGCAACGGCTATTTTCA	TGGTGGAGATGTTATGGTATGGTC
<i>Dm-nub1</i>	867bp	CACCTTTTAATAAAAAACATAAAGTA	ATATGGGTATGTGTCATTTGT
<i>Dm-nub2</i>	1337bp	CACCATTGTAGAAGACGCAGCTTTG	TTGCTATTTAAATTTTGATGG
<i>Dm-nub3</i>	512bp	CACCAAACGAGCTCGATCCGCGGCT	TTTCATAAAGCTCATAAAGGT
<i>Dm-nub2a</i>	500bp	CACCATTGTAGAAGACGCAGCTTTG	TGGATATTAGTGCAAAACGCT
<i>Dm-nub2b</i>	500bp	CACCCCTGCCGCTCCTCCTGCCCAT	ACAATTATTGTCACAAAACA
<i>Dm-nub2c</i>	479bp	CACCAATTACTTATTTTCATTATA	TTGCTATTTAAATTTTGATGG
pFGUM	3379bp	ACTGGGCCGCCCCCTTCGTCCTCAAGAATTCG	ACTGGGCCGCGCCTCCGGAACATAAT
<i>mCherry</i>	362bp	CGACATCCCCGACTACTTGA	TGATGTTGACGTTGTAGGCG

Table S5. Primers used in this study

Table S6. The list of differentially accessible FARIE peaks. (attached separately)